

DUNCAN LIBRARY
NAVAL POSTGRADUATE SCHOOL
MONTEREY, CALIFORNIA 93943

NAVAL POSTGRADUATE SCHOOL

Monterey, California



THESIS

REVIEW, IMPLEMENTATION AND TEST OF THE
QAZ1D COMPUTATIONAL METHOD WITH A
VIEW TO WAVE ROTOR APPLICATIONS

by

Thomas F. Salacka

December 1985

Thesis Advisor:

Ray P. Shreeve

Approved for public release; distribution is unlimited

Prepared for: Naval Air Systems Command
Washington, DC 20361

T226826

NAVAL POSTGRADUATE SCHOOL
Monterey, California

Rear Admiral Robert H. Shumaker
Superintendent

David A. Schradly
Provost

This thesis prepared in conjunction with research sponsored in part by the Naval Air Systems Command, Washington, DC, under Air Task #A310310E/186A/WR024-03-001.

Reproduction of all or part of this report is authorized.

Released By:

REPORT DOCUMENTATION PAGE

REPORT SECURITY CLASSIFICATION Unclassified			1b. RESTRICTIVE MARKINGS			
SECURITY CLASSIFICATION AUTHORITY			3. DISTRIBUTION/AVAILABILITY OF REPORT Approved for public release; distribution is unlimited			
DECLASSIFICATION/DOWNGRADING SCHEDULE						
PERFORMING ORGANIZATION REPORT NUMBER(S) NPS67-85-012			5. MONITORING ORGANIZATION REPORT NUMBER(S) NPS67-85-012			
NAME OF PERFORMING ORGANIZATION Naval Postgraduate School		6b. OFFICE SYMBOL (If applicable) Code 67	7a. NAME OF MONITORING ORGANIZATION Naval Postgraduate School			
ADDRESS (City, State, and ZIP Code) Monterey, California 93943-5100			7b. ADDRESS (City, State, and ZIP Code) Monterey, California 93943-5100			
NAME OF FUNDING/SPONSORING ORGANIZATION Naval Air Systems Command		8b. OFFICE SYMBOL (If applicable) Air 310E	9. PROCUREMENT INSTRUMENT IDENTIFICATION NUMBER N0001985WR 51147			
ADDRESS (City, State, and ZIP Code) Washington, D.C. 20361			10. SOURCE OF FUNDING NUMBERS			
			PROGRAM ELEMENT NO 61153N	PROJECT NO WR024	TASK NO. 03	WORK UNIT ACCESSION NO 001
TITLE (Include Security Classification) VIEW, IMPLEMENTATION AND TEST OF THE QAZ1D COMPUTATIONAL METHOD WITH A VIEW TO WAVE ROTOR APPLICATIONS						
PERSONAL AUTHOR(S) Slacka, Thomas F.						
TYPE OF REPORT Master's Thesis		13b. TIME COVERED FROM _____ TO _____		14. DATE OF REPORT (Year, Month, Day) 1985, December		15. PAGE COUNT 119
SUPPLEMENTARY NOTATION						
COSATI CODES			18. SUBJECT TERMS (Continue on reverse if necessary and identify by block number) QAZ1D; Wave Rotor; Computational Fluid Dynamics; Euler			
FIELD	GROUP	SUB-GROUP				
ABSTRACT (Continue on reverse if necessary and identify by block number) The QAZ1D method is redeveloped in detail and implemented in a first order, one-dimensional FORTRAN program, EULER-1. The program is tested on the shock tube problem and results are presented for various computational meshes and initial conditions. Based on good results of the EULER-1 code, recommendations are made for future						
DISTRIBUTION/AVAILABILITY OF ABSTRACT <input checked="" type="checkbox"/> UNCLASSIFIED/UNLIMITED <input type="checkbox"/> SAME AS RPT <input type="checkbox"/> DTIC USERS			21. ABSTRACT SECURITY CLASSIFICATION Unclassified			
NAME OF RESPONSIBLE INDIVIDUAL Prof. Ray P. Shreeve			22b. TELEPHONE (Include Area Code) (408) 646-2593		22c. OFFICE SYMBOL Code 67Sf	

#19 - ABSTRACT - (CONTINUED)

extensions and testing to validate the suitability
of the QAZ1D method for wave rotor applications.

Approved for public release; distribution is unlimited.

Review, Implementation and Test of the
QAZ1D Computational Method with a
View to Wave Rotor Applications

by

Thomas Francis Salacka
Lieutenant, United States Navy
B.S., United States Naval Academy, 1977

Submitted in partial fulfillment of the
requirements for the degree of

MASTER OF SCIENCE IN AERONAUTICAL ENGINEERING

from the

NAVAL POSTGRADUATE SCHOOL
December 1985

ABSTRACT

The QAZ1D method is redeveloped in detail and implemented in a first order, one-dimensional FORTRAN program, EULER-1. The program is tested on the shock tube problem and results are presented for various computational meshes and initial conditions. Based on good results of the EULER-1 code, recommendations are made for future extensions and testing to validate the suitability of the QAZ1D method for wave rotor applications.

TABLE OF CONTENTS

I.	INTRODUCTION -----	13
II.	THE QAZ1D METHOD -----	17
	A. OVERVIEW -----	17
	B. DEVELOPMENT OF THE EQUATIONS -----	17
	C. SOLUTION METHOD -----	22
	D. DISCONTINUITIES IN THE FLOW -----	25
III.	DESCRIPTION OF FORTRAN PROGRAM "EULER-1" -----	30
	A. MACHINE AND LANGUAGE -----	30
	B. CONVENTIONS AND BASIC STRUCTURE -----	30
	C. SUBROUTINE DESCRIPTIONS -----	33
	D. CAPABILITIES AND LIMITATIONS -----	40
IV.	TEST RESULTS -----	42
V.	DISCUSSION -----	52
	A. RESULTS -----	52
	B. SPECIAL CONSIDERATIONS -----	52
	C. SUITABILITY FOR WAVE ROTOR APPLICATIONS -----	54
VI.	CONCLUSIONS -----	56
APPENDIX A:	DERIVATION OF THE GOVERNING EQUATIONS FOR THREE-DIMENSIONAL INVISCID FLOW (WITH AREA CHANGE) -----	57
APPENDIX B:	USING EULER-1 ON THE NPS VM/CMS SYSTEM ----	92
APPENDIX C:	EULER-1 FORTRAN CODE -----	95
LIST OF REFERENCES	-----	115
INITIAL DISTRIBUTION LIST	-----	116

LIST OF FIGURES

1.	Solution Procedure in the Space-Time Domain -----	23
2.	Shock Wave with High Pressure to the Left -----	27
3.	Shock Wave with High Pressure to the Right -----	27
4.	$(Q_A - Q_B)/A_B$ vs W -----	27
5.	EULER-1 Flowchart -----	31
6.	"RSHOCK" Case -----	36
7.	EULER-1 Results for Pressure Ratio 5, with Shock Tracking -----	44
8.	Exact Solution Comparison for Pressure Ratio 5, with Shock Tracking -----	45
9.	EULER-1 Results for Pressure Ratio 1.3, with Shock Tracking -----	46
10.	Exact Solution Comparison for Pressure Ratio 1.3, with Shock Tracking -----	47
11.	Course Mesh Solution for Pressure Ratio 5 -----	48
12.	Fine Mesh Solution for Pressure Ratio 5 -----	49
13.	EULER-1 Results for Pressure Ratio 5, without Shock Tracking -----	50
14.	Exact Solution Comparison for Pressure Ratio 5, without Shock Tracking -----	51

TABLE OF SYMBOLS

Below are two tables of symbols. The first table lists all the symbols which occur in the text and, where applicable, their FORTRAN counterparts used in the EULER-1 code. The second table lists the remaining symbols used in the EULER-1 code which were not listed in the first table. Both tables are in alphabetical order.

SYMBOLS USED IN THE TEXT

<u>Text</u>	<u>EULER-1</u>	<u>Definition</u>
A	A	Speed of sound
P	PRESS	Static pressure
Q	QQ	Modified Riemann variable ($Q = q + AS$)
q	Q	Absolute velocity magnitude
Q_R		Reversible heat transferred
R	RR	Modified Riemann variable ($R = q - AS$)
R_G		Gas constant
S	S	A modified form of entropy
$\hat{1}_{s,n,m}$		Unit vectors in the s, n, and m directions
T	TEMP	Static Temperature
t	T	Time
u	U	Velocity magnitude relative to a steady shock wave
V_s	VS	Shock wave velocity
W	W	Mach number relative to a steady shock wave

\overline{w}		Vector of the principle variables, Q,R,S
\overline{z}	Z(K)	Vector of the right hand sides of the governing equations
λ	LMD(K)	The characteristic trajectories in the space-time plane (q+A, q-A, q)
Δ		Small spatial change
δ		Small change with respect to time
θ, ϕ		Flow angles with respect to reference coordinate planes
ρ	DENS	Density
γ	G	Ratio of specific heats

ADDITIONAL SYMBOLS USED IN EULER-1

<u>Symbol</u>	<u>Definition</u>
A	Suffix which denotes the left side of a discontinuity (may be any variable)
ABAR(K)	The average value of A between the limits of integration of Z(K)
B	Suffix which denotes the right side of a discontinuity (may be any variable)
AR	The ratio of the sound speeds across a shock, (high/low)
COUNT	A counter for the number of time steps
DARRAY	The array of density values to be plotted by the graphics routines
DEL**H	The change in the variable ** in going from node I to node I+1 [**(I+1) - **(I)]
DELX(K)	The distance from the point where the K th characteristic crosses the known time level to the I th node, measured positive to the right
DEL**I,	The change in the variable ** in going from node I-1 to node I [**(I) - **(I-1)]

DLCD	The exact value of the density to the left of a right propagating contact discontinuity in the Riemann problem
DLSH	The exact value of the density to the left of a right propagating shock in the Riemann problem
DLTA**	A prefix which indicates the spatial change in ** over one time step
DQ	The change in the velocity magnitude across a shock, (high-low)
DR	The ratio of the density across a shock, (low/high)
EE	A value which indicates the precision to which the characteristics are to be calculated
E(K)	The computed error in the calculation of the characteristics
GRAPHS	Parameter which controls the type of output produced by EULER-1. 0 = Tabular, 1 = Plot of Q, S, pressure and density, 2 = Comparison of density with exact solution
G1	$1/(G-1)$
G2	$2/(G-1)$
H	The non-dimensional value of one spatial interval $1/(N-1)$
I	Subscript which denotes the spatial node
**INT(K)	The interpolated value of ** at the point on the known time level where the K^{th} characteristic crosses
INTEG(K)	The result of integrating $Z(K)$
I2(L)	The node to the right of discontinuity L
J	The time level
JSTOP	The number of time levels desired to be computed
K	A subscript which indicates the characteristic being dealt with. 1 = Q+A 2 = Q-A 3 = Q

L	A subscript which denotes the type of discontinuity. 1 = shock 2 = contact discontinuity 3 = head of rarefaction wave 4 = tail or rarefaction wave
M	Parameter which controls the types of discontinuities which EULER-1 tracks. 1 = shocks only. 2 = shocks and contact discontinuities
N	The number of nodes in the computational grid
NEW**	A temporary storage location for variables ** updated in time
PARRAY	The array of densities plotted by the graphics routines
PR	The ratio of pressures across a shock, (high/low)
PRI	The initial pressure ratio across the diaphragm (high/low)
*PRIM(K)	Suffix which indicates the spatial derivative of * at the present time level, where * is either A or Q
QARRAY	The array of velocities to be plotted by the graphics routines
QLI	The initial value of the velocity to the left of the diaphragm
QRI	The initial value of the velocity to the right of the diaphragm
QQJO	The measured change in the Riemann variable QQ across a shock (high-low)
QQJE	The change in the Riemann variable QQ across a shock calculated analytically (high-low)
SIGMA(L,J)	Discontinuity locations. J = 1 indicates the known time level and J = 2 indicates the unknown time level
STEP	The change in the primary variables with respect to time during one time step (= QQ, RR, S)

SARRAY	The array of entropy values to be plotted by the graphics routines
SKIP	The number of time steps between outputs
TRI	The initial temperature ratio across the diaphragm (high/low)
VCDE	The exact velocity of the contact discontinuity
VHEAD	The exact velocity of the head of the rarefaction wave
VTAIL	The exact velocity of the tail of the rarefaction wave
VS	The shock wave velocity computed by EULER-1
VSE	The exact velocity of the shock wave
X	The non-dimensional spatial position
XARRAY	The array of node locations used by the graphics routines
XINIT	The initial location of the discontinuities. Used to calculate the exact solution
X2(L)	The position of the node to the right of a discontinuity

ACKNOWLEDGMENT

Thanks to my wife, Kathy, for her support and encouragement, to Augie Verhoff, for his personal assistance, to Atul Mathur, for his availability and assistance, and to Ray Shreeve, for making this an enjoyable and worthwhile learning experience.

I. INTRODUCTION

A program is underway at the Naval Postgraduate School's (NPS) Turbopropulsion Laboratory to evaluate the wave rotor concept. The wave rotor, operating as a component in a gas turbine engine, uses unsteady wave propagation in tube-like passages to compress incoming air before it goes to the combustion chamber. The combustion chamber output is routed back to the rotor to create the unsteady waves. Thus the rather simple rotor, with "partial admission" inlet and outlet ports, acts both as a compressor and as a turbine. The alternation of hot and cool gases through the same hardware aids cooling and allows higher operating (cycle) temperatures to be used. The interaction of the hot and cool gases within the passages of the wave rotor through the wave patterns that are created pose a difficult problem. The work underway aims to develop and validate preliminary design and performance analysis tools.

One of the tools needed is a computer program which can be used to construct wave interactions in a design process and then accurately predict the performance of the design. Until efficient and accurate methods of solving the full Navier-Stokes equations for unsteady turbulent flows are developed, the design program will be based initially on the solution of the unsteady Euler equations and a method devised to represent losses. Once the program is developed, it must

be verified against experiment. This is the overall goal of the present program in which a wave rotor apparatus has been assembled and methods of measuring the unsteady pressures and temperatures are being developed concurrently with the computational effort.

Three different approaches to the solution of the unsteady Euler equations were examined in the overall program. First, Eidelman developed a two-dimensional code based on the Godunov method of solution [Ref. 1] and applied the code to examine unsteady wave propagation in ducts [Ref. 2] and the process of port opening to wave rotor passages [Ref. 3]. A summary of Eidelman's work is given in Reference 4. While the method is conservative and does not require the introduction of artificial viscosity, the extension from one to two dimensions is not rigorous when shock waves are present, and computational times with the present code are quite long. The extension to include viscous effects would require a separate treatment of the boundary layer.

Second, Mathur developed a one-dimensional code based on the Random Choice Method (RCM) of solution [Ref. 5]. Somewhat similar to the Godunov method, in that the solution is based on solving the Riemann problem within each grid cell at each time step, the RCM approach results in very sharp discontinuities which can be tracked easily. This is particularly useful in constructing wave rotor cycles, in which the position of the gas-gas interface is equally as important as the position

of the compression and expansion waves. The code is therefore valuable in the preliminary design process, to examine suitable port arrangements, and the gas properties at the ports, for a given task. Unfortunately, an extension to two-dimensional and/or viscous flow can not be made rigorously.

The third approach was followed in the present work. The QAZ1D method for compressible inviscid flow computations developed by Verhoff and O'Neil [Ref. 6] was implemented to generate a one-dimensional unsteady Euler code with the goal of evaluating the suitability of the approach for wave rotor applications. Some advantages of the QAZ1D method were recognized as being the following:

1. The method is based on the use of characteristics. Such methods can model wave propagation accurately.
2. The use of a natural streamline coordinate system eases the difficult task of computing with two and three dimensional grids.
3. The equations are written in a form which allows a straightforward extension to viscous flows.
4. Codes for computing internal, steady, two-dimensional flows in the presence of shocks, and simple internal viscous flows, have been generated quickly without significant development problems [Ref. 6].

In the work reported herein, a one-dimensional FORTRAN code based on the QAZ1D method was developed using the NPS IBM370-3033 computer and subsequently exercised on the shock tube test problem. In reporting the work, first, in Section II and Appendix A, a complete account is given of the derivation and non-dimensionalization of the governing equations.

In Section III, a FORTRAN code, EULER-1, is described. Its operation on the NPS computer, and the listing of the code, are given in Appendix B and Appendix C, respectively. Results of applying the code to the shock tube test problem are given in Section IV. Difficulties encountered in the implementation of the method and additional comments are given in Section V, and conclusions are given in Section VI.

II. THE QAZ1D METHOD

A. OVERVIEW

The QAZ1D method uses Riemann-like variables with a modified entropy term in their definitions, to express the Euler equations in a natural streamline coordinate system. The resulting partial differential equations (PDE), when cast along the characteristic trajectories in the space-time domain, reduce to a system of ordinary differential equations (ODE) which may be solved explicitly. The advantage in using the modified Riemann variables is that they are less affected by discontinuities in the flow than are the standard Riemann variables. Since the equations are not valid across discontinuities which cause irreversible losses, such discontinuities must be located and treated with special logic in the numerical formulation.

In the following presentation, the reader's familiarity with the method of characteristics is assumed.

B. DEVELOPMENT OF THE EQUATIONS

This section presents the governing equations and outlines their development. A rigorous derivation of the equations is presented in Appendix A.

1. The Coordinate System

The natural streamline coordinate system (s, n, m) , is shown in Fig. A-1 relative to a fixed rectangular cartesian

system (x,y,z). The (s,n,m) system is a right-hand orthogonal system which undergoes curvilinear translation as it moves with a fluid particle along a streamline. The coordinate system is described in detail in Appendix A.

2. Variables

The modified Riemann variables, or "extended Riemann variables" [Ref. 6:p. 1], are defined as

$$\begin{aligned} Q &= q + AS \\ R &= q - AS \end{aligned} \tag{1}$$

where q is the velocity magnitude, A is the speed of sound and S is the modified entropy defined in terms of pressure and density as

$$S = \frac{R_G}{\gamma(\gamma-1)} [2\gamma - \ln(P/\rho^\gamma)] \tag{2}$$

The modified entropy relation is the result of defining the entropy change, dS , to be given by

$$dS = - \frac{1}{\gamma} \frac{dQ_R}{T} \tag{3}$$

where dQ_R is the heat required to be added in a reversible process between the same end states, T is the temperature and γ is the ratio of specific heats.

3. Conservation of Mass

By applying the continuity equation to a differential stream tube of variable cross sectional area, in natural coordinates, and ignoring all third order and higher derivatives, one obtains

$$\frac{\partial \rho}{\partial t} + q \frac{\partial \rho}{\partial s} + \rho \frac{\partial q}{\partial s} + \rho q \left[\frac{\partial \theta}{\partial n} + \cos \theta \frac{\partial \phi}{\partial m} \right] = 0 \quad (4)$$

where q is the velocity, ρ is the density, s is the stream-wise spatial dimension, and θ and ϕ are the flow angles as defined in Fig. A-1 of Appendix A.

4. Conservation of Momentum

Applying the vector form of the momentum conservation law in natural coordinates, the equation of motion for inviscid flow becomes

$$\begin{aligned} & \hat{i}_s \left[\rho \frac{\partial q}{\partial t} + \rho q \frac{\partial q}{\partial s} + \frac{\partial P}{\partial s} \right] \\ & + \hat{i}_n \left[\rho q \frac{\partial \theta}{\partial t} + \rho q^2 \frac{\partial \theta}{\partial s} + \frac{\partial P}{\partial n} \right] \\ & + \hat{i}_m \left[\rho q \cos \theta \frac{\partial \phi}{\partial t} + \rho q^2 \cos \theta \frac{\partial \phi}{\partial s} + \frac{\partial P}{\partial m} \right] = 0 \end{aligned} \quad (5)$$

5. The Conservation of Energy

In the absence of friction and heat conduction, and outside of discontinuities (through which irreversible changes consistent with mass, momentum and energy conservation are permitted), energy conservation is equivalent to the

statement that the entropy of a fluid particle does not change. In the natural coordinate system, therefore

$$\frac{dS}{dt} = \frac{\partial S}{\partial t} + q \frac{\partial S}{\partial s} = 0 \quad (6)$$

Equation (6) will not be valid across shock waves or contact surfaces between gases having different states.

6. Transformation to a Useful Form

Equations (4) and (5) are first expressed in terms of the primary variables q , A , S , and the flow angles. Using the definition of sound speed in a perfect gas

$$A^2 = \gamma P / \rho \quad (7)$$

Eq. (4) becomes

$$\frac{\partial A}{\partial t} + q \frac{\partial A}{\partial s} + \frac{\gamma-1}{2} A \frac{\partial q}{\partial s} + q A \frac{\gamma-1}{2} \left[\frac{\partial \theta}{\partial n} + \cos \theta \frac{\partial \phi}{\partial m} \right] = 0 \quad (8)$$

With Eq. (3), the equation of state for a perfect gas, and the first law of thermodynamics, Eq. (5) gives

$$\begin{aligned} \frac{\partial q}{\partial t} + q \frac{\partial q}{\partial s} + \frac{2A}{\gamma-1} \frac{\partial A}{\partial s} + A^2 \frac{\partial S}{\partial s} &= 0 \\ \frac{\partial \theta}{\partial t} + q \frac{\partial \theta}{\partial s} &= - \frac{A^2}{\gamma q} \frac{\partial \ln P}{\partial n} \\ \frac{\partial \phi}{\partial t} + q \frac{\partial \phi}{\partial s} &= - \frac{A^2}{\gamma q \cos \theta} \frac{\partial \ln P}{\partial m} \end{aligned} \quad (9)$$

Equations (6), (8) and (9) constitute the system of P.D.E.'s which describe the unsteady isentropic flow of a perfect gas in natural coordinates. Since third order terms were neglected in the conservation of mass, the system is only accurate to second order.

The system of P.D.E.'s is now transformed into a system of O.D.E.'s along the characteristic trajectories. In general, if w is a function of (s,t) , then

$$dw = \frac{\partial w}{\partial s} ds + \frac{\partial w}{\partial t} dt$$

or

$$\frac{dw}{dt} = \frac{\partial w}{\partial s} \left(\frac{ds}{dt} \right) + \frac{\partial w}{\partial t} \quad (10)$$

where (ds/dt) describes the "characteristic" direction in the (s,t) plane along which Eq. (10) gives the rate of change of the parameter w . After the appropriate algebra and the introduction of Eq. (1), the final system of equations becomes

$$\left. \begin{aligned} \frac{\partial Q}{\partial t} + (q+A) \frac{\partial Q}{\partial s} &= - \frac{\gamma-1}{2} A \left(S - \frac{2}{\gamma-1} \right) \left[\frac{\partial}{\partial s} \left(q - \frac{2}{\gamma-1} A \right) \right] \\ &\quad - \frac{\gamma-1}{2} q A S \left[\frac{\partial \theta}{\partial n} + \cos \theta \frac{\partial \phi}{\partial m} \right] \\ \frac{\partial R}{\partial t} + (q-A) \frac{\partial R}{\partial s} &= + \frac{\gamma-1}{2} A \left(S - \frac{2}{\gamma-1} \right) \left[\frac{\partial}{\partial s} \left(q + \frac{2}{\gamma-1} A \right) \right] \\ &\quad + \frac{\gamma-1}{2} q A S \left[\frac{\partial \theta}{\partial n} + \cos \theta \frac{\partial \phi}{\partial m} \right] \end{aligned} \right\} \quad (11)$$

$$\frac{\partial S}{\partial t} + q \frac{\partial S}{\partial s} = 0$$

$$\frac{\partial \theta}{\partial t} + q \frac{\partial \theta}{\partial s} = - \frac{A^2}{\gamma q} \frac{\partial \ln P}{\partial n}$$

$$\frac{\partial \phi}{\partial t} + q \frac{\partial \phi}{\partial s} = - \frac{A^2}{\gamma q \cos \theta} \frac{\partial \ln P}{\partial m}$$

The characteristic directions in the space-time plane are clearly $q+A$, $q-A$, and q .

C. SOLUTION METHOD

Equation (11) may be expressed as

$$\frac{\partial \bar{w}}{\partial t} + [\lambda] \frac{\partial \bar{w}}{\partial s} = \bar{z} \quad (12)$$

or along the λ directions as

$$\frac{d\bar{w}}{dt} = \bar{z} \quad (13)$$

where the vectors are defined as

$$\bar{w} = \begin{Bmatrix} Q \\ R \\ S \\ \theta \\ \phi \end{Bmatrix} \quad [\lambda] = \begin{bmatrix} q+A & & & & \\ & q-A & & & \\ & & q & & \\ & & & q & \\ & & & & q \end{bmatrix} \quad \bar{z} = \text{right hand side of Eq. (11)}$$

A trajectory in the space-time domain is illustrated in Fig. 1,

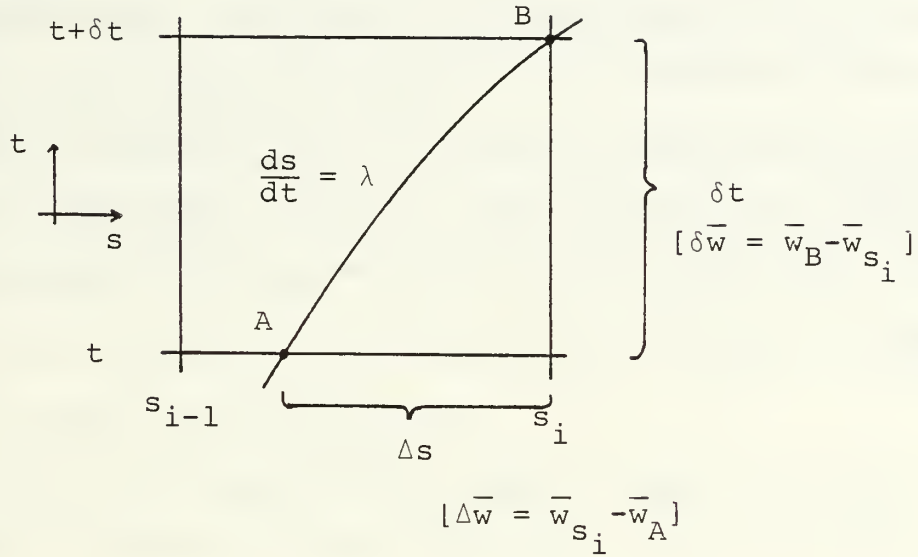


Figure 1. Solution Procedure in the Space-Time Domain

which shows an infinitesimal interval of space between two "nodes" of the computational mesh.

For the change in \bar{w} from A to B along the trajectory with slope λ ,

$$\begin{aligned}
 \int_t^{t+\delta t} \bar{z} \, dt &= \bar{w}_B - \bar{w}_A \\
 &= [\bar{w}_B - \bar{w}_{s_i}] + [\bar{w}_{s_i} - \bar{w}_A] \\
 &= \delta \bar{w} + \Delta \bar{w}
 \end{aligned}$$

where $\delta\bar{w}$ denotes the change due to time at a fixed location and $\Delta\bar{w}$ denotes the change due to displacement at a fixed time, for the characteristic trajectory. The essence of the solution procedure is to calculate the change in the variables at each spatial node during the differential time interval, so that the step to the next time level can be made. In other words, $\delta\bar{w}$ must be calculated at each node using

$$\delta\bar{w} = -\Delta\bar{w} + \int_t^{t+\delta t} \bar{z} \, dt \quad (14)$$

Since all the information at time level t is known, the position of A can be determined by an iterative procedure based on λ and $\Delta\bar{w}$ can be calculated by interpolation. The line integral can be evaluated by transforming the integral to a purely spatial integral using $\lambda = ds/dt$. Thus

$$\int_t^{t+\delta t} \bar{z} \, dt = \int_A^B \frac{\bar{z}}{\lambda} \, ds = \int_{s_i+\Delta s}^{s_i} \frac{\bar{z}}{\lambda} \, ds$$

and the integral can be evaluated by any one of several numerical methods. Thus, the variables at each node can be updated in time using Eq. (14) and the process repeated.

D. DISCONTINUITIES IN THE FLOW

There are several types of discontinuities that must be considered. They are gradient discontinuities, contact discontinuities and shock waves.

Gradient discontinuities are characteristic of the head and tail of rarefaction waves, the collision of two shocks and the interaction of a shock and a contact discontinuity. Across such a gradient, the derivatives of velocity, pressure and sound speed are discontinuous.

A contact discontinuity is caused by the interaction of two shocks of opposite family and when a shock overtakes a shock of the same family. Entropy and sound speed are discontinuous at a contact discontinuity.

Across shock waves, velocity, pressure, density and entropy are discontinuous [Ref. 7].

Since Eq. (11) is not valid across discontinuities, additional logic is required in the numerical procedure to model flows which contain discontinuities. The method presented in Reference 6 for making a correction in the case of shock waves will give good accuracy in problems where the solution is converging to a steady state condition but will not give accurate results during the transient portion of such problems or for problems with only unsteady solutions. In the case of applications to the wave rotor, it would certainly be necessary to know the locations of the contact surfaces between the

hot and cool gases as well as the locations of the shock and expansion waves.

The methods used in the present work to correct for discontinuities are those of Moretti [Ref. 7]. The present discussion will be limited to the treatment of shock waves. The method makes use of the analytical relationship between the change in the Riemann variables across a shock and the incoming Mach number relative to the shock wave (W) which is illustrated in Figs. 2 and 3. The relation is used to determine the shock speed and to transform the problem to a steady case which can be handled using normal shock relations. For the situation depicted in Fig. 2 of a shock propagating to the right with velocity V_s into air with velocity q_B , and with the high pressure side to the left, where A denotes the left side of the shock and B the right,

$$W = -\frac{u_B}{A_B} = \frac{-(q_B - V_s)}{A_B} \quad (15)$$

If the pressure and density are non-dimensionalized by the values on the low pressure side of the shock, the change in the extended Riemann variable Q is given by

$$\begin{aligned} \frac{Q_A - Q_B}{A_B} &= \frac{2(W^2 - 1)}{(\gamma + 1)W} + \frac{2}{\gamma - 1} \left[\frac{A_A}{A_B} - 1 \right] \\ &\quad - \frac{A_A}{A_B} \left[\frac{1}{\gamma(\gamma - 1)} \right] \ln \left\{ \left[\frac{2\gamma}{\gamma + 1} W^2 - \left(\frac{\gamma - 1}{\gamma + 1} \right) \right] \left[\frac{(\gamma - 1)W^2 + 2}{(\gamma + 1)W^2} \right]^\gamma \right\} \end{aligned} \quad (16)$$

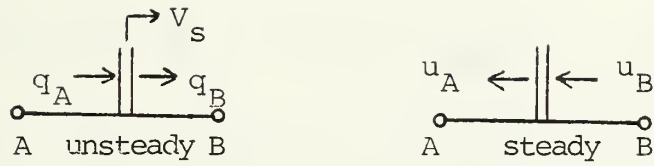


Figure 2. Shock Wave with High Pressure to the Left



Figure 3. Shock Wave with High Pressure to the Right

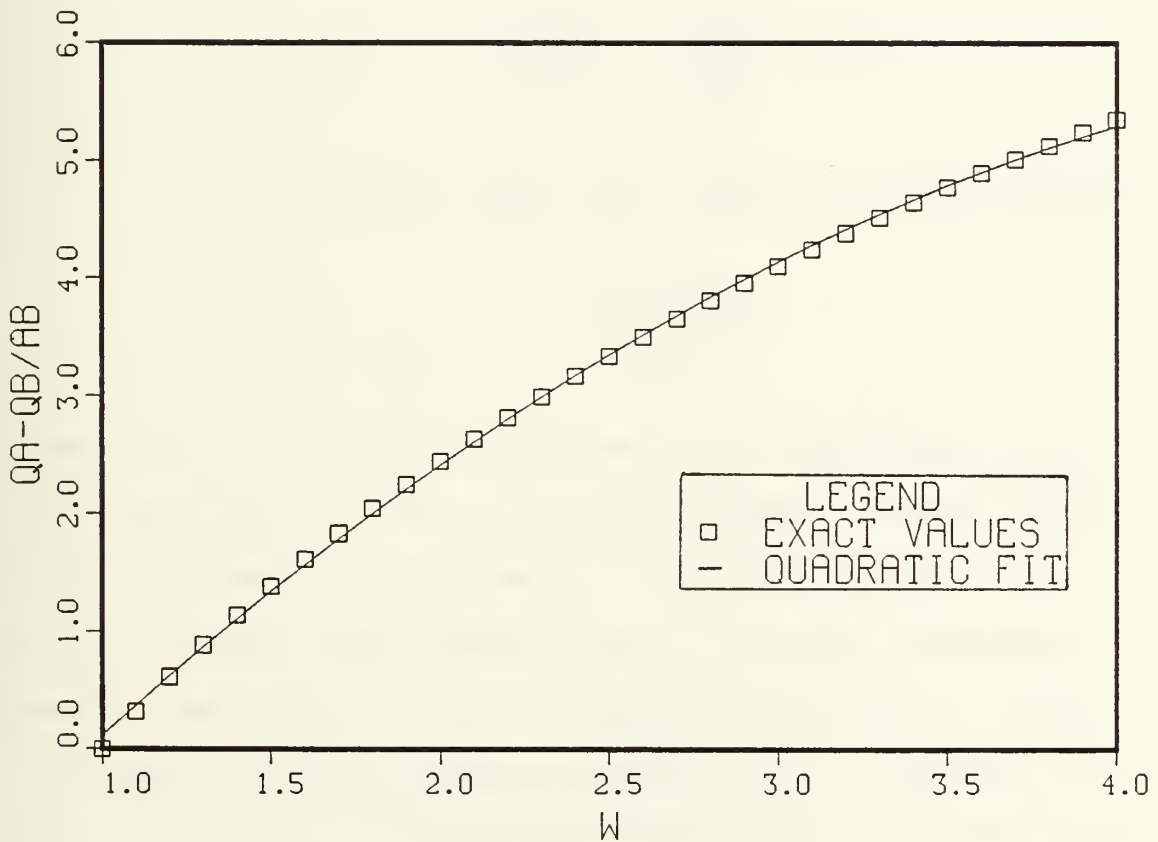


Figure 4. $(Q_A - Q_B)/A_B$ vs W

where

$$\frac{A_A}{A_B} = \frac{1}{(\gamma+1)W} \{ 2(\gamma-1) \left[1 + \frac{\gamma-1}{2} W^2 \right] \left[\frac{2\gamma}{\gamma-1} W^2 - 1 \right] \}^{1/2}$$

This exact relationship can be approximated by the polynomial

$$\frac{Q_A - Q_B}{A_B} = -2.7574 + 3.1573W - 0.2863W^2 \quad (17)$$

as illustrated in Fig. 4 over a shock strength range of 1.0 to 4.0. It should be noted that if the high pressure side were to the right, as in Fig. 3, Eq. (15) would become

$$W = \frac{u_A}{A_A} = \frac{q_A - V_s}{A_A}$$

and the left side of Eq. (16) would become

$$\frac{R_A - R_B}{A_A}$$

The procedure then, is to measure the change in Q across an interval where a shock is known to exist. This value, call it ΔQ_m , is used in Eq. (17) to get an approximation for the corresponding value of W and then the exact value of ΔQ , call it ΔQ_E , is calculated using Eq. (16). If the exact value of ΔQ is not equal to the value measured across the shock, a new value, ΔQ , is calculated according to

$$\Delta Q_{i+1} = \Delta Q_i + (\Delta Q_m - \Delta Q_E)$$

and entered into Eq. (17) to obtain another value of W . When the exact value of ΔQ calculated from Eq. (16) equals the measured value of ΔQ , W is known to be correct and the normal shock relations can be used to calculate the values at node A. Also, V_s can be calculated from Eq. (15) and used to track the shock during the next time interval.

III. DESCRIPTION OF FORTRAN PROGRAM "EULER-1"

A. MACHINE AND LANGUAGE

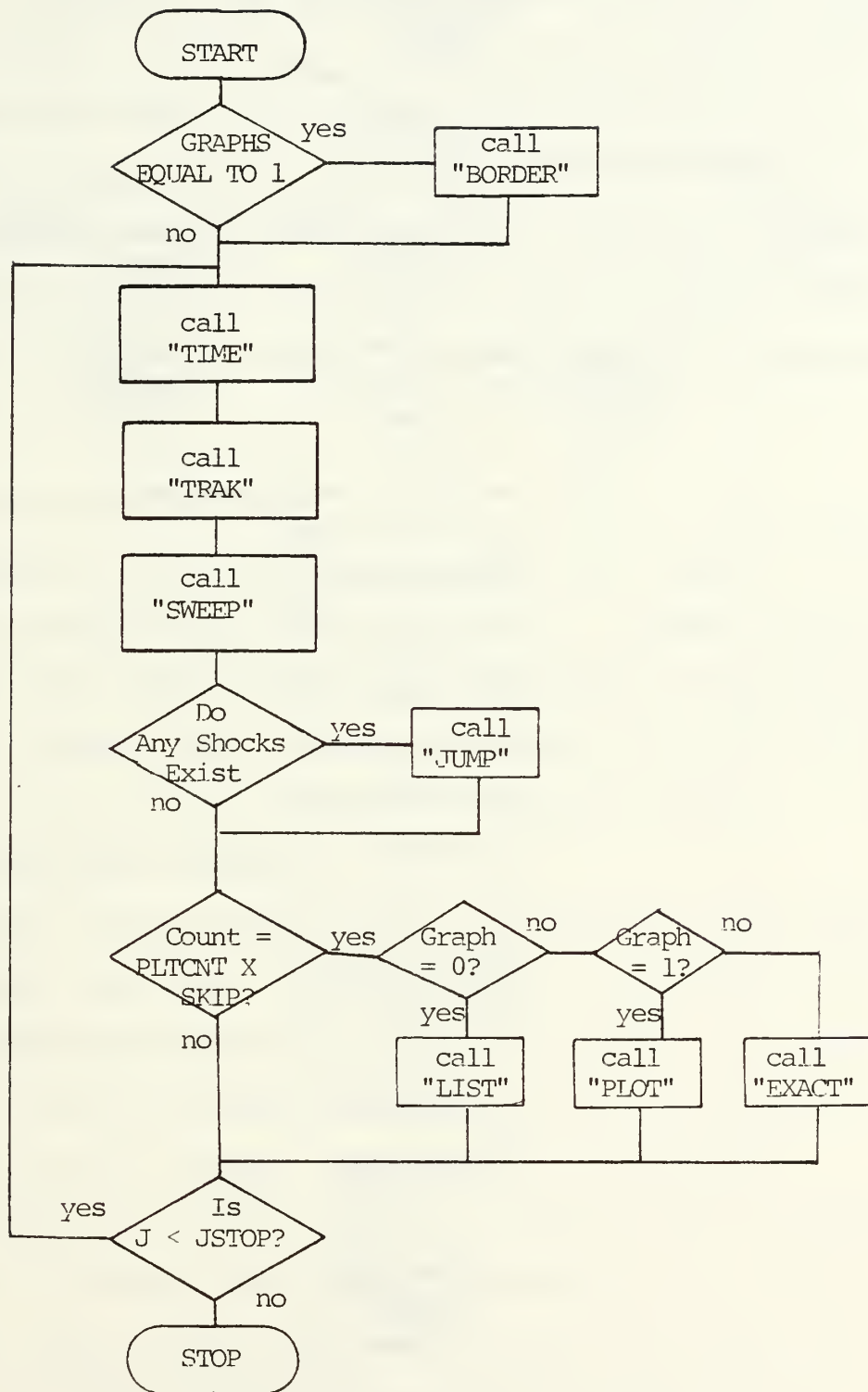
The EULER-1 program is written in VS FORTRAN and runs on an IBM 3033, System 370 computer, however the code is simple and small enough to enter and run on a mini or micro computer in a Basic language if one is willing to accept significantly longer run times. Table 1 at the end of this section is a summary of the editable parameters and their effect on the program.

B. CONVENTIONS AND BASIC STRUCTURE

EULER-1 is a first-order one-dimensional code using an evenly spaced numerical grid. All values are double precision except those used in the graphics routines which are rounded to single precision.

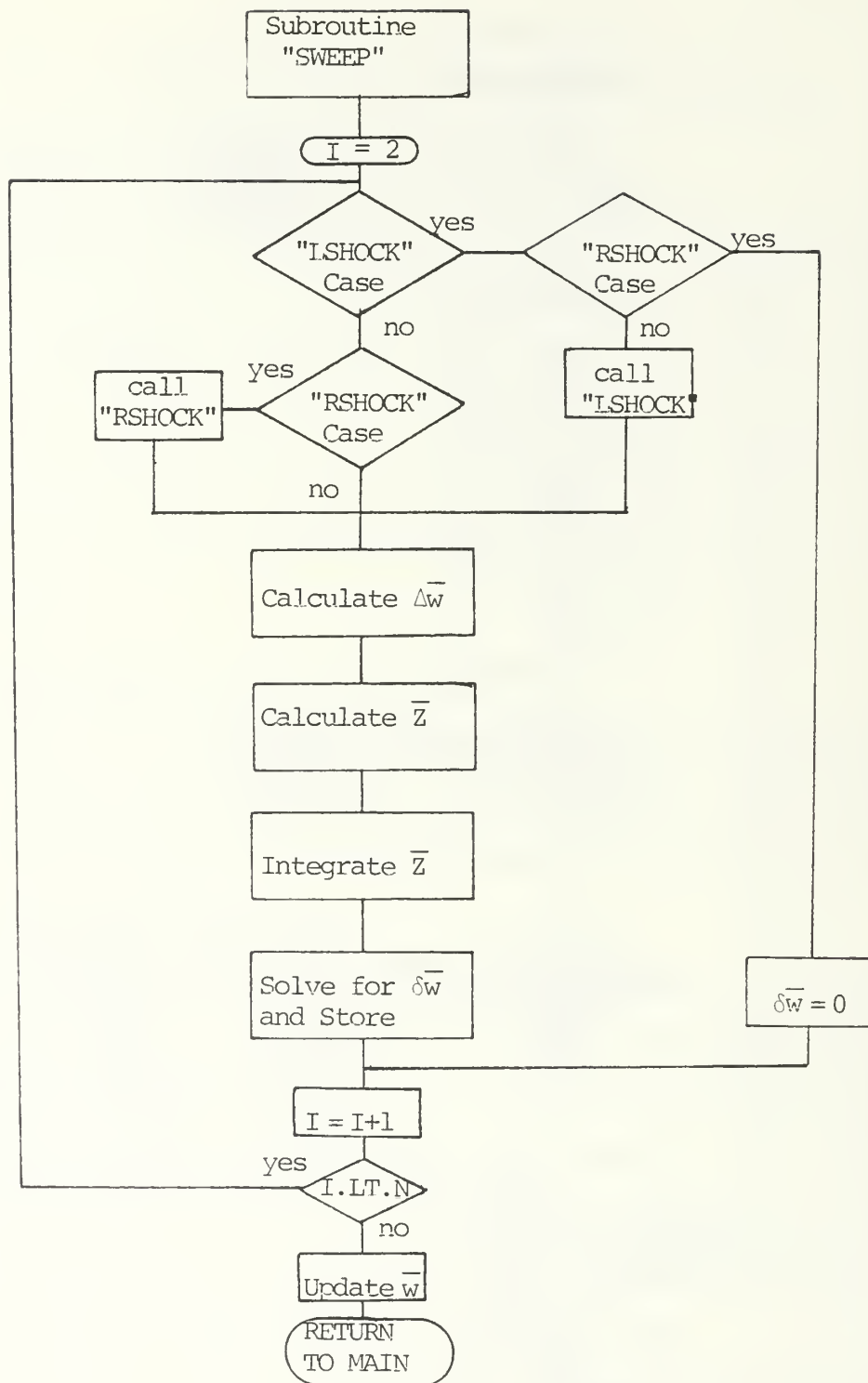
Each subroutine has its own variables space. In other words, variables are not shared in common throughout the program but must be passed to the subroutine being called by the calling routine. In all cases, however, the variables have the same name in both the called and the calling routine so there should be no confusion. This was done so that arrays could be dimensioned at execution time.

The program, depicted in Fig. 5, is structured around a main routine which serves as a user input area, sets up the problem and calls five subroutines to solve the problem and



a) Main Program

Figure 5. EULER-1 Flowchart



b) "SWEEP" Subroutine

Figure 5. (Continued)

output the solution. The five subroutines are "TIME," "TRAK," "SWEEP," "JUMP" and then one of several output routines depending on user desires. Output options include two types of graphical displays, "PLOT" and "EXACT," and one tabular listing routine, "LIST." When "PLOT" is selected, "BORDER" is automatically called to set up the plotting area. There are two other subroutines, "RSHOCK" and "LSHOCK," which are called by "SWEEP" as needed.

C. SUBROUTINE DESCRIPTIONS

In general, each subroutine begins with a heading followed by variable definitions where appropriate, variable declarations and array dimensioning. Most variables are defined in the "MAIN" routine and only those variables which were not are defined in the subroutines where they are used.

1. The "MAIN" Routine

This routine forms the main structure of the program and includes a heading, an extensive list of variable definitions, a user input area, the necessary statements to make the initial value assignments to variables, and the call statements for the various subroutines.

The input area is those lines of the program (145-175) where the user edits the program to establish the initial conditions, mesh size, termination criteria and output options.

The initial conditions which may be modified are the pressure, temperature and density ratios across the diaphragm, the initial velocity of the fluid on each side of the

diaphragm, and the value of gamma (which must be the same for both sides).

All velocities are non-dimensionalized by the initial sound speed on the low pressure side of the diaphragm and pressures and densities are non-dimensionalized by their initial values on the low pressure side of the diaphragm.

The mesh size may be set at any odd number and the arrays in the user input area must be dimensioned as such.

The criteria for program termination is the number of time steps computed, which the user selects.

The output options are determined by the value of the variable GRAPHS. A value of zero results in a call to "LIST" which writes to file 9 on the user's permanent disk, a tabular listing of the variable arrays and discontinuity locations. A value of 1 results in a call to "BORDER" and "PLOT" which create a plot of the pressure, density, velocity and entropy distributions as in Fig. 7. A value of 2 results in a call to "EXACT" which creates a plot of the density distribution compared to the exact solution as in Fig. 8. The exact values to be plotted must be entered in the user input area, they are not calculated by the program. A more detailed description of the various outputs is found under the appropriate subroutine description. The frequency with which output is created is controlled by the variable SKIP which is the number of time steps between calls to output routines.

2. The "TIME" Routine

The maximum allowable time step is governed by the CFL condition. Simply stated, this means that the time step must be small enough so that the characteristic trajectories remain within one spatial interval during the time interval. The minimum time step is calculated by computing

$$\text{Delt} = H/\text{ABS}[Q+A]$$

at every node, where H is the spatial interval, and selecting the minimum value of Delt.

3. The "TRAK" Routine

Shock locations at the unknown time level are determined by computing the shock speed at the known time level, as outlined in Section 2, and multiplying by the time interval computed by "TIME." The time step is reduced, if necessary, to limit shock travel to one spatial interval. The node immediately to the right of the shock (upstream) is flagged for later use by "SWEEP" and "JUMP."

In calculating the shock speed, the assumption is made that the conditions immediately adjacent to the shock are the same as the conditions at the nodes to the left and right of the shock.

4. The "SWEEP" Routine

The "SWEEP" routine makes the necessary calculations to solve Eq. (14). This involves interpolation at the known

time level for the values of $\Delta \bar{w}$, calculation of \bar{z} , and integration of \bar{z} for each node.

To calculate $\Delta \bar{w}$, the assumption is made that the characteristic trajectories are straight lines. An initial guess of the characteristic slope (λ) is made and by forcing the characteristic to pass through the node at point B in Fig. 1, $\Delta s = \lambda \times \Delta t$. The values of q and A at point A are found by interpolation and the slope of the characteristic is then calculated using the values of q and A at point A. This slope is compared with the initial guess and if the two are not in agreement, the procedure is iterated until they converge. Once Δs is accurately determined, the values of $\Delta \bar{w}$ can be calculated by interpolation. Linear interpolation is used in the present version of EULER-1. This procedure is carried out for each characteristic at each node.

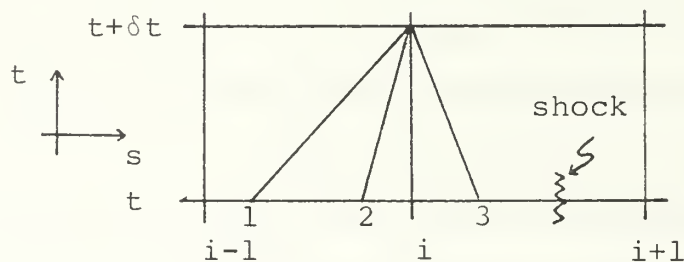


Figure 6. "RSHOCK" Case

A deviation from the above procedure is necessary in the case where a shock exists in the spatial interval to the left or right of the current node. When a shock exists to

the right, and the flow is subsonic, as in Fig. 6, care must be taken not to interpolate for point 3 based on the slope between points I+1 and I, which would not be accurate due to the discontinuity. In such a case "RSHOCK" is called and the interpolation is based on the slope between point I and I-1. Similarly, when the shock is to the left of the current node, "LSHOCK" is called and the interpolation is based on the slope between I+1 and I.

The calculation of \bar{z} includes the calculation of spatial derivatives of q and A for characteristics 1 and 3 of Fig. 6. In general, the derivatives associated with characteristic 3 are forward differenced and those associated with characteristic 1 are backward differenced in keeping with the principle of domain of dependence. If the flow is supersonic or if a shock exists to the right of the current node, all derivatives are backward differenced. If a shock exists to the left of the current node, all derivatives are forward differenced. Once the derivatives are known, \bar{z} is calculated from Eq. (11) using the average value of A between points 1 and I or 3 and I as appropriate. Since the derivatives are linear, this results in an average value of \bar{z} over the same interval.

The integration of \bar{z} is transformed from a time to a spatial integration as described in Section II and the trapezoidal rule is used to carry out the integration. In EULER-1, this has been done in one step using the average value of \bar{z} described above.

Equation (14) is then solved by addition of $\Delta \bar{w}$ and the results of the integration, and the resulting $\delta \bar{w}$ is stored until all nodes are calculated. After all nodes have been calculated, the variable arrays (\bar{w}) are updated for the next time interval.

5. The "LSHOCK" Routine

As discussed above, the "LSHOCK" routine modifies the basic EULER-1 procedure at an interior node when a shock exists to the left of the node. Interpolation of quantities to the left of the node are computed based on the derivatives of the quantities to the right of the node. Although this assumes that the derivatives do not change between adjacent spatial intervals, it is necessary to avoid taking derivatives across discontinuities in the flow.

6. The "RSHOCK" Routine

Similar to "LSHOCK," "RSHOCK" bases interpolations of quantities to the right of the node on the derivatives of the quantities to the left of the node when a shock exists to the right of the node.

7. The "JUMP" Routine

The "JUMP" routine is used to calculate the conditions downstream of a stationary shock as described in Section II. If a shock is known to have crossed a spatial node during a time interval, which is known once "TRAK" has been called for that time interval, the entire "SWEEP" sequence is skipped for the node which was crossed by the shock and the conditions at

that node are determined using the normal shock relations. Note that the node in question is the node downstream of the stationary shock. As in "TRACK," it is assumed that the conditions at the nodes upstream and downstream of the shock are the same as the conditions immediately adjacent to the shock.

8. The Output Routines

There are four subroutines which produce various types of output as the user desires. "BORDER" and "PLOT" produce a graphical presentation of the pressure, density, velocity and entropy distributions at selected time levels as seen for example, in Fig. 7. "EXACT" produces a plot of the density distribution at one selected time interval and compares it with the exact solution as shown in Fig. 8. At selected time levels, "LIST" produces a tabular listing of the Riemann variables, modified entropy, pressure, density and velocity distributions, elapsed time, shock speed and discontinuity locations. The listing is written to the user's permanent storage disk.

When the value of GRAPHS is set equal to one in the "MAIN" routine, "BORDER" is called once to set up the plot axis, labels, and headings. "PLOT" is called every SKIP time steps to draw the four distribution curves.

When the value of GRAPHS is set equal to two, "EXACT" is called every SKIP time steps to plot the density distribution compared with the exact solution computed at six points of interest. The points are the two end points, which

are simply the initial conditions, the head and tail of the rarefaction wave, the point just left of the contact surface and the point just left of the shock. The spatial locations of these points are computed by "EXACT" based on the elapsed time and the known values of the wave velocities entered in the "MAIN" routine. The exact values of the densities at these points must also be entered in the "MAIN" routine.

When the value of GRAPHS is set equal to zero, the tabular listing as described above is sent to the user's disk. No graphical output is created.

D. CAPABILITIES AND LIMITATIONS

The present version of EULER-1 is set up to solve a shock tube problem with a single centered diaphragm. Boundary conditions for the ends of the tube have not been incorporated so the problem must be stopped before the waves reach the end of the tube.

The left side of the diaphragm is the high pressure side. The program will not run with the right side as the high pressure side without changes to some of the shock correction logic.

The user may select any odd number of grid points limited only by the amount of memory available.

The program tracks shock waves and makes shock jump calculations at the appropriate locations but the program can also run without the shock tracking feature and jump calculations if so desired with some smearing of the shock discontinuity and complete loss of entropy change across the shock.

TABLE 1
LIST OF EDITABLE PARAMETERS

<u>Parameter</u>	<u>Function</u>
N	Number of grid points
M	Controls which discontinuities are tracked 1 = Shocks only 2 = Shocks and contact surfaces
GRAPHS	Controls the form of the output 0 = Tabular listing 1 = Pressure, density, velocity, entropy plot 2 = Exact solution comparison for density
SKIP	Number of time steps between output calls
JSTOP	Number of time steps calculated
TRI	Initial temperature ratio
PRI	Initial pressure ratio
DRI	Initial density ratio
QLI	Initial velocity left of the diaphragm
QRI	Initial velocity right of the diaphragm
G	Ratio of specific heats

IV. TEST RESULTS

EULER-1 was tested on the Riemann shock tube problem. The initial conditions and the coarseness of the computational mesh were varied. Additionally, one run was made without the shock tracking and correction features.

Figures 7 and 8 show the results for initial pressure and density ratios of 5, uniform temperature and with the air initially at rest, using a grid of 101 points. The exact, analytically predicted conditions are also shown in Fig. 8. It can be seen that all wave velocities are correctly computed and the shock is defined within one interval. The rarefaction waves are slightly smeared and the contact surface is greatly smeared. A slight transient instability to the right of the diaphragm is noticeable, particularly in the plots of pressure and velocity.

Figures 9 and 10 show results for initial pressure and density ratios of 1.3. The shock is still well defined in the correct interval and the contact surface is not as badly smeared as in Fig. 8. There is a loss of accuracy however, with respect to the tail of the rarefraction wave.

Figure 11 shows the results of the original problem with a grid of 51 points. As might be expected with a coarser mesh, the discontinuities are less sharply defined although it is clear that the wave velocities are accurately computed.

Figure 12 shows the results for the original problem with a grid of 901 points. It can be seen that the EULER-1 solution closely approximates the exact solution.

Figures 13 and 14 show the result of running the original problem without the shock tracking and correcting features. Note that the shock position is incorrectly computed and it is smeared slightly. Also note in Fig. 13, the lack of any change in modified entropy across the shock.

Run time for the 101 point mesh is 0.00049 seconds per node per time step. The results for Fig. 7 took 50 time steps for a total time of 2.46 seconds. For the 901 point mesh, the run time decreased to 0.00023 seconds per node per time step due to the less frequent use of the shock tracking and correction routines per node calculated. The results for Fig. 12 took 470 time steps for a total time of 71.85 seconds.

SHOCK TUBE RESULTS

FIRST ORDER $N = 101$
DENSITY RATIO = 5 TEMP RATIO = 1
PRESSURE RATIO = 5

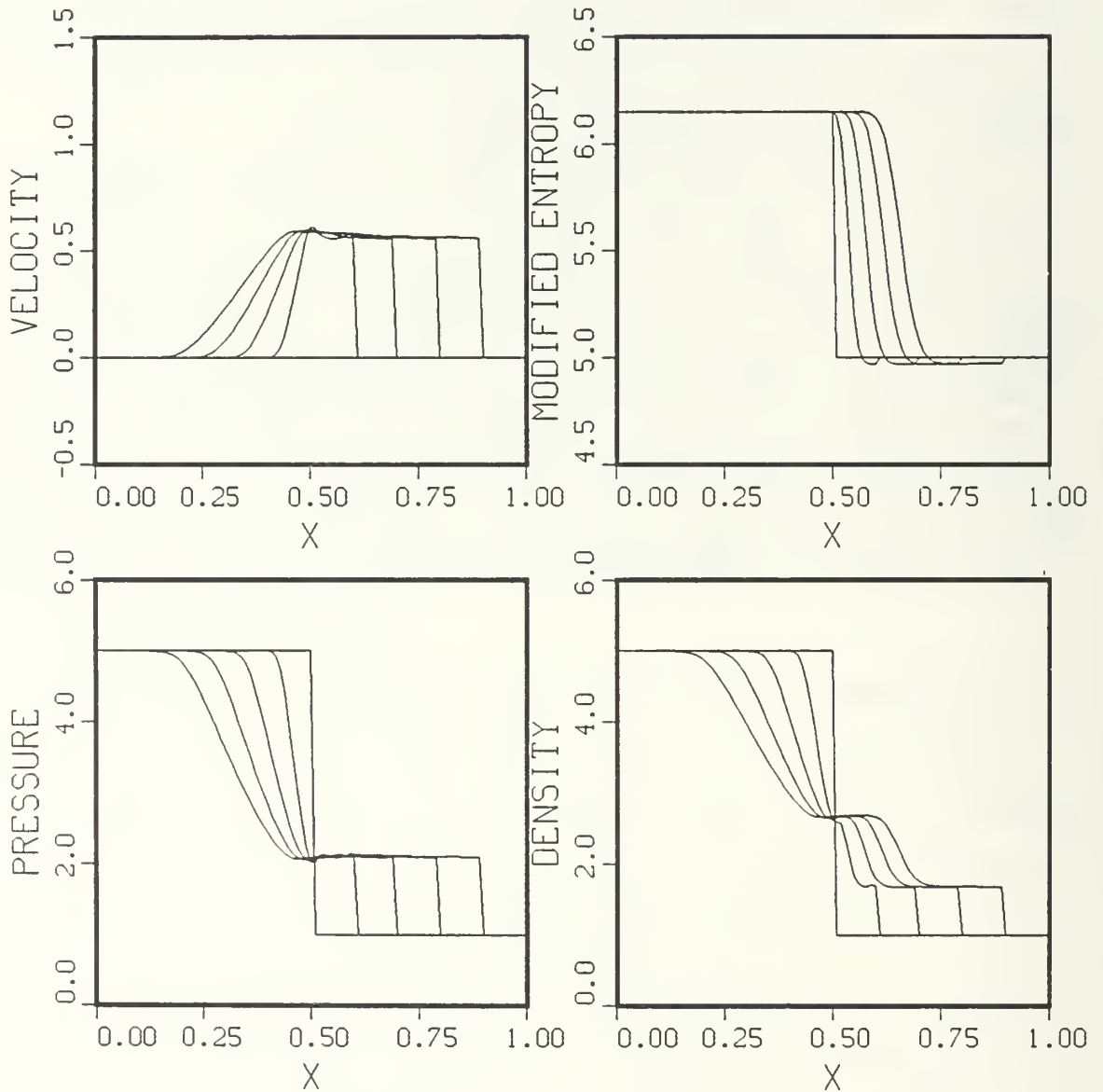


Figure 7. EULER-1 Results for Pressure Ratio 5 with Shock Tracking

DENSITY DISTRIBUTION
 FIRST ORDER N = 101
 DENSITY RATIO = 5 TEMP RATIO = 1
 PRESSURE RATIO = 5

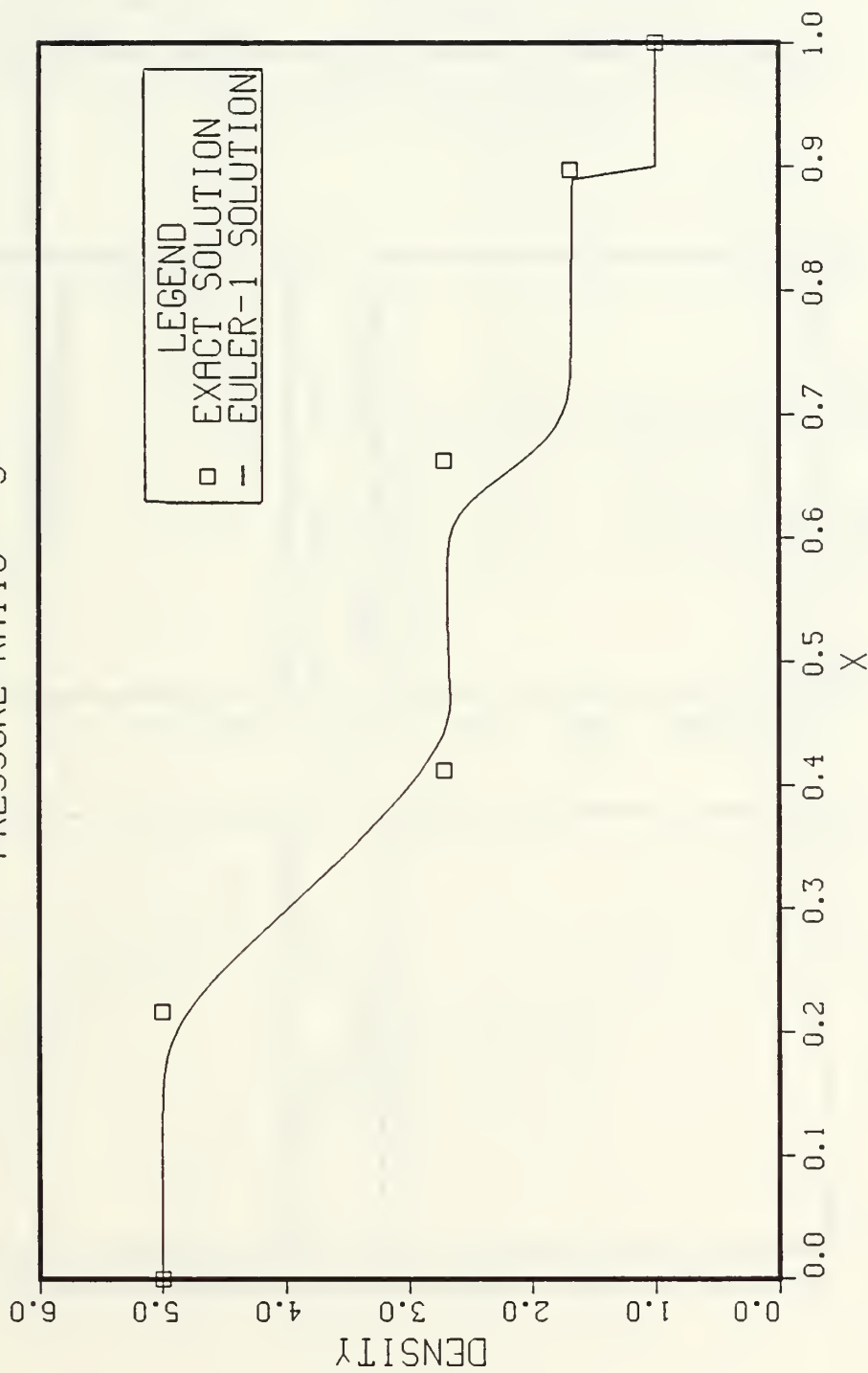


Figure 8. Exact Solution Comparison for Pressure Ratio 5, with Shock Tracking

SHOCK TUBE RESULTS
FIRST ORDER $N = 101$
DENSITY RATIO = 1.3 TEMP RATIO = 1
PRESSURE RATIO = 1.3

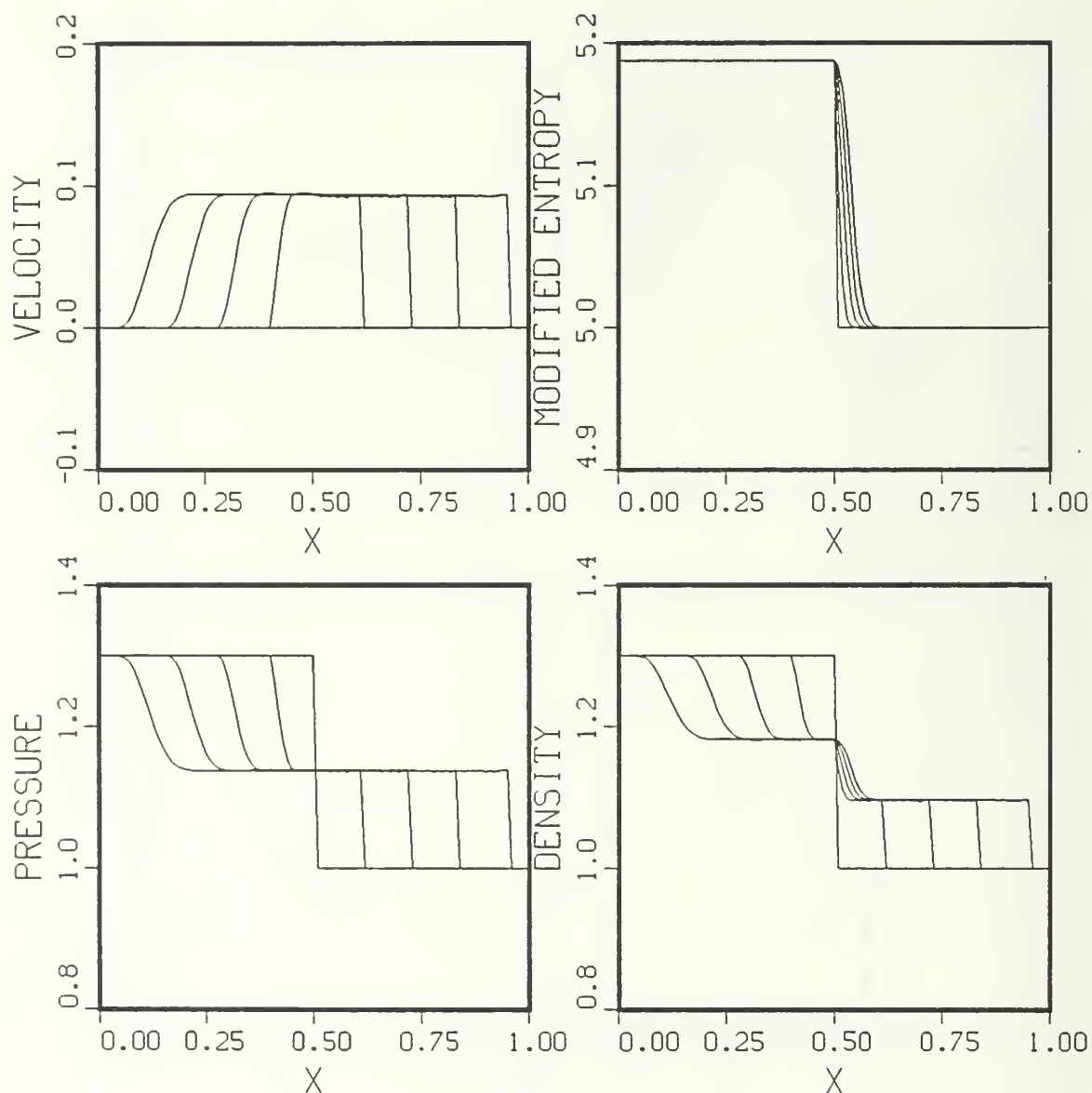


Figure 9. EULER-1 Results for Pressure Ratio 1.3 with Shock Tracking

DENSITY DISTRIBUTION
 FIRST ORDER N = 101
 DENSITY RATIO = 1.3 TEMP RATIO = 1
 PRESSURE RATIO = 1.3

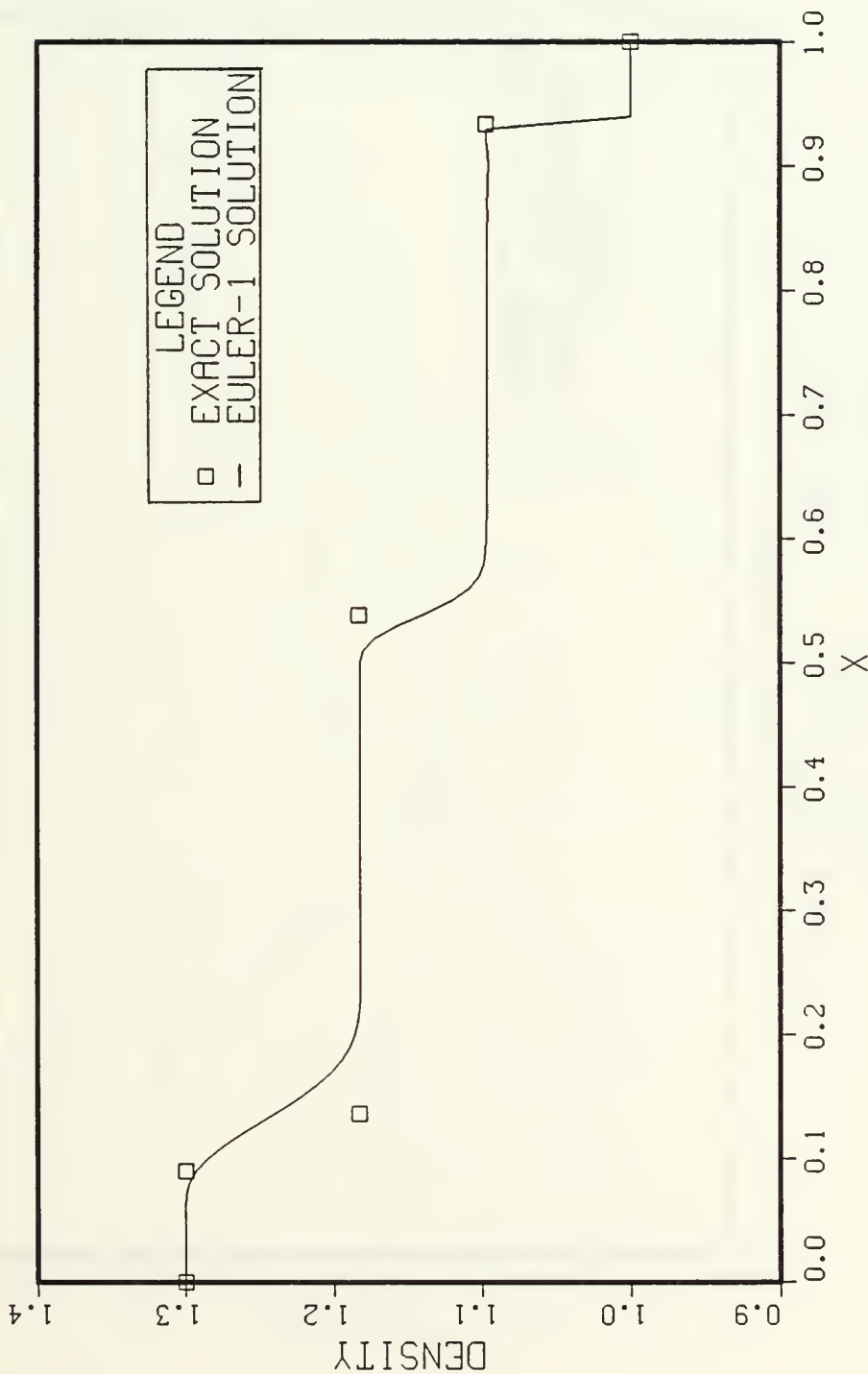


Figure 10. Exact Solution Comparison for Pressure Ratio 1.3, with Shock Tracking

DENSITY DISTRIBUTION

FIRST ORDER N = 51

DENSITY RATIO = 5 TEMP RATIO = 1

PRESSURE RATIO = 5

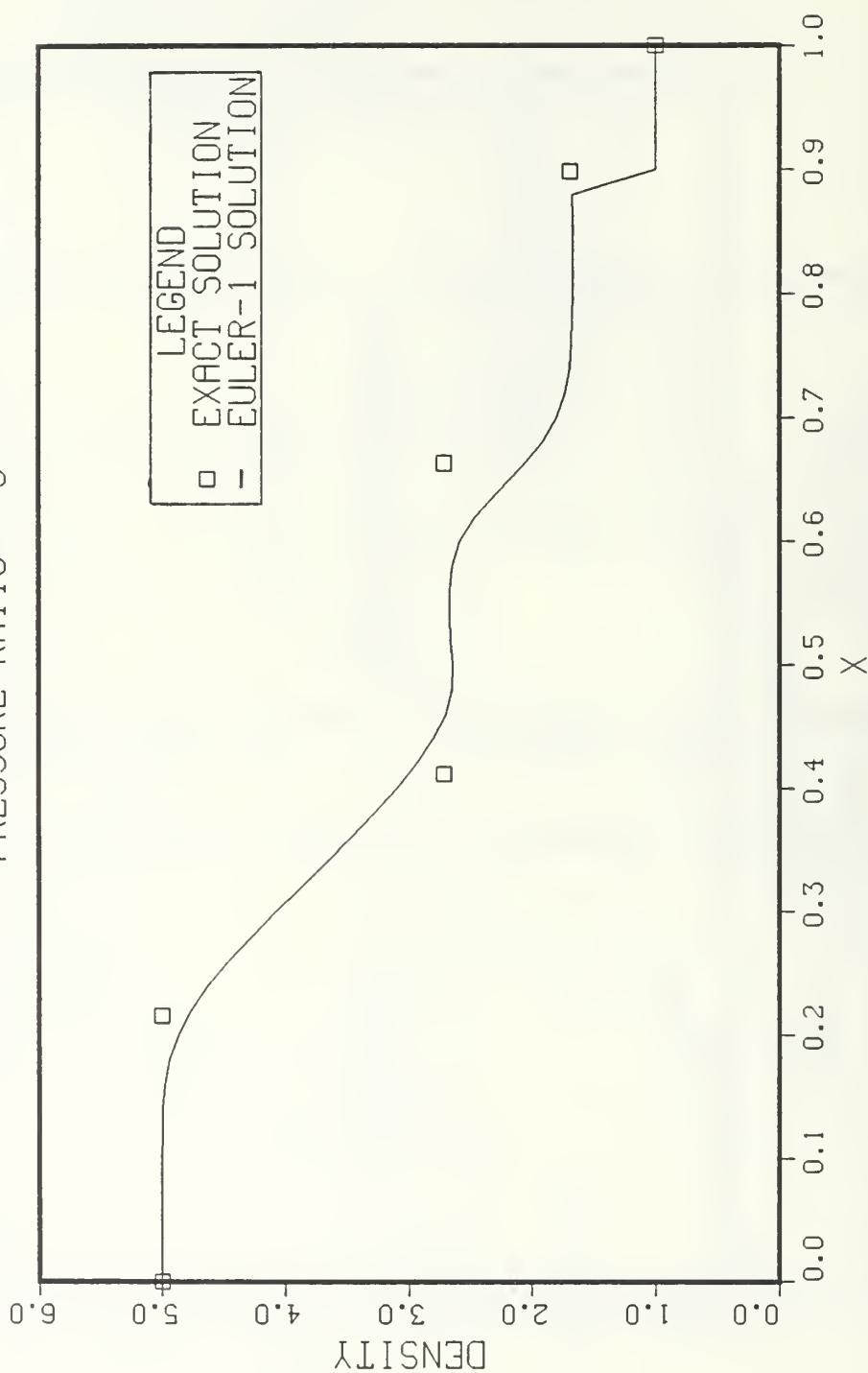


Figure 11. Course Mesh Solution for Pressure Ratio 5

DENSITY DISTRIBUTION
 FIRST ORDER N = 901
 DENSITY RATIO = 5 TEMP RATIO = 1
 PRESSURE RATIO = 5

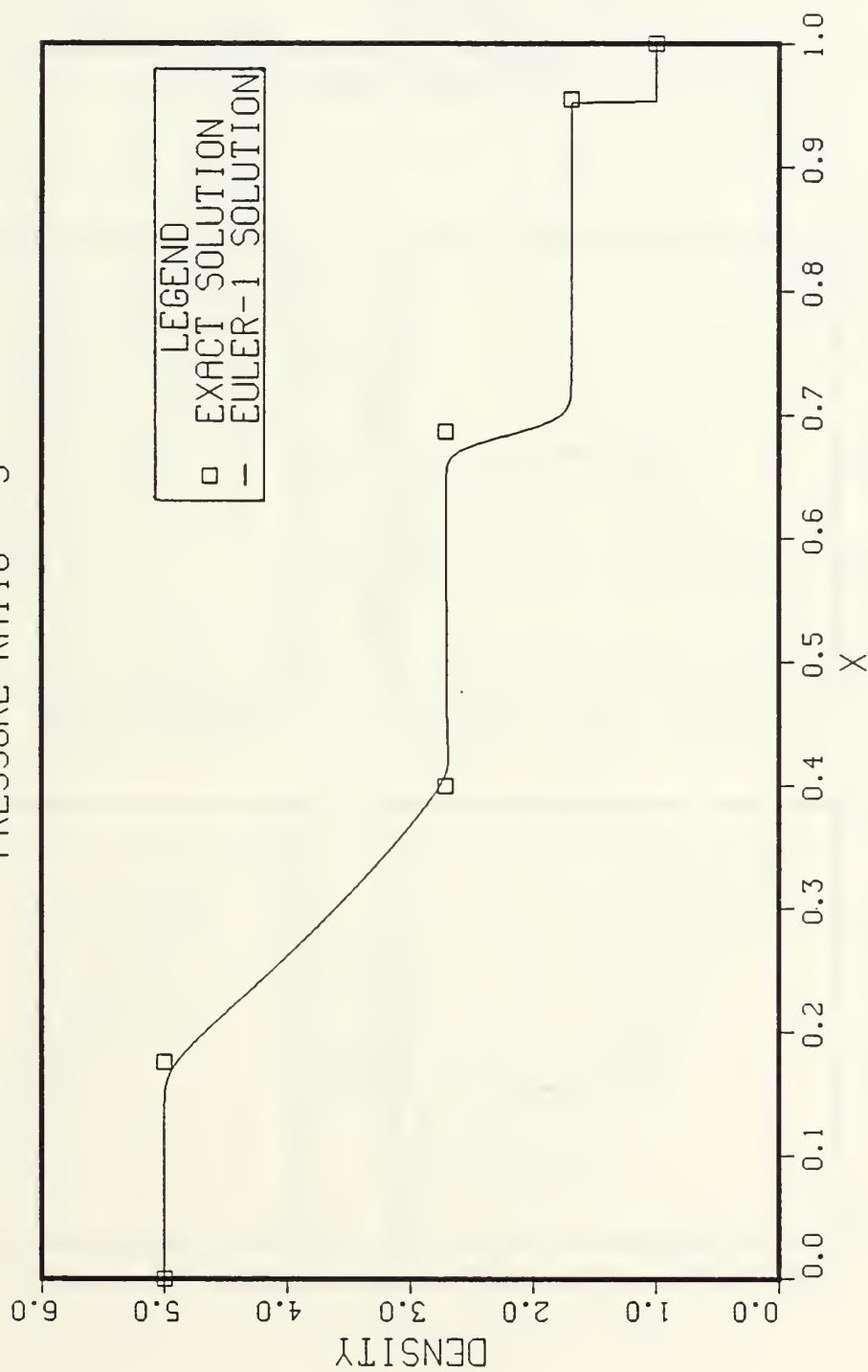


Figure 12. Fine Mesh Solution for Pressure Ratio 5

SHOCK TUBE RESULTS

FIRST ORDER $N = 101$
 DENSITY RATIO = 5 TEMP RATIO = 1
 PRESSURE RATIO = 5

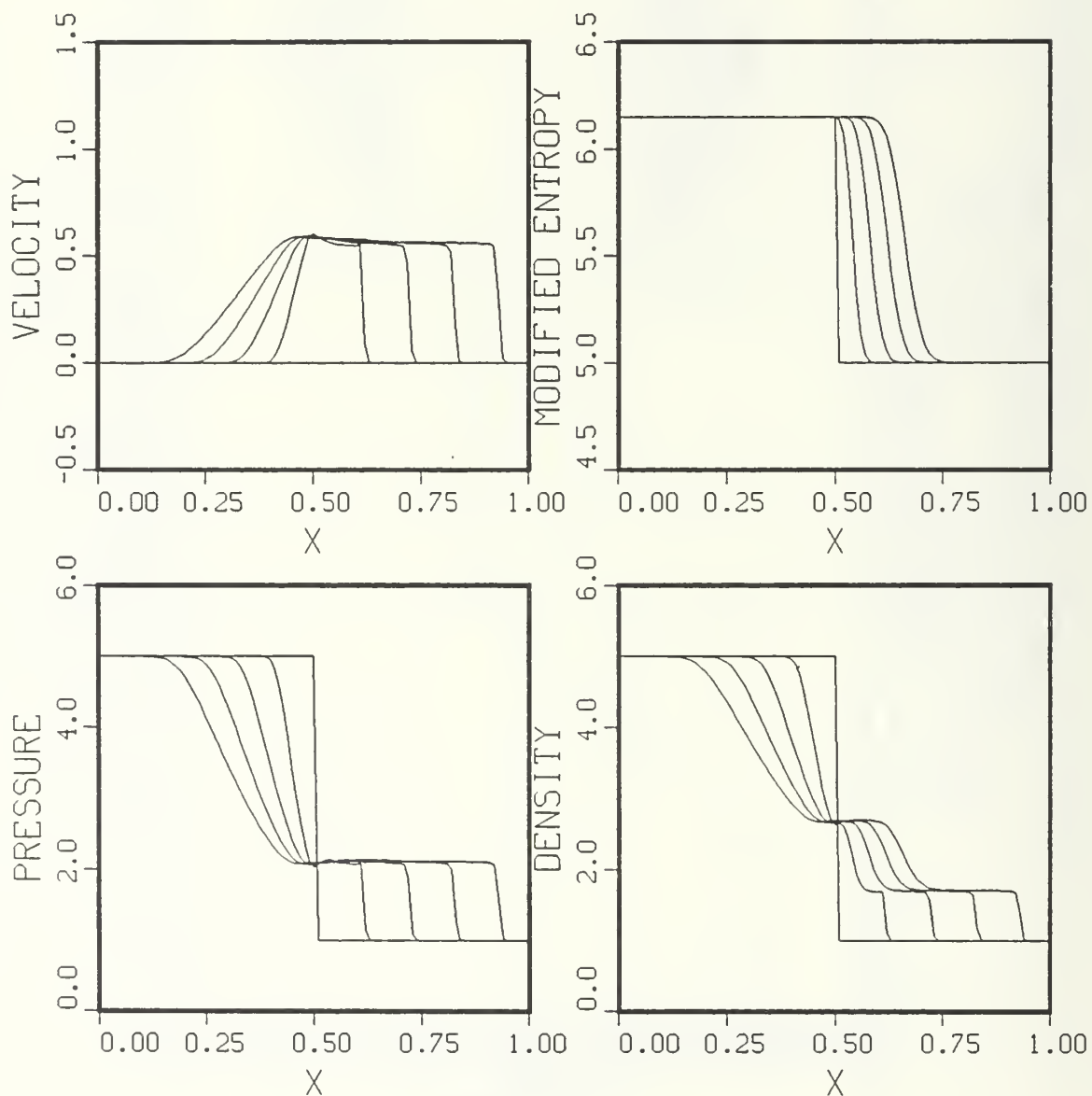


Figure 13. EULER-1 Results for Pressure Ratio 5 without Shock Tracking

DENSITY DISTRIBUTION
 FIRST ORDER N = 101
 DENSITY RATIO = 5 TEMP RATIO = 1
 PRESSURE RATIO = 5

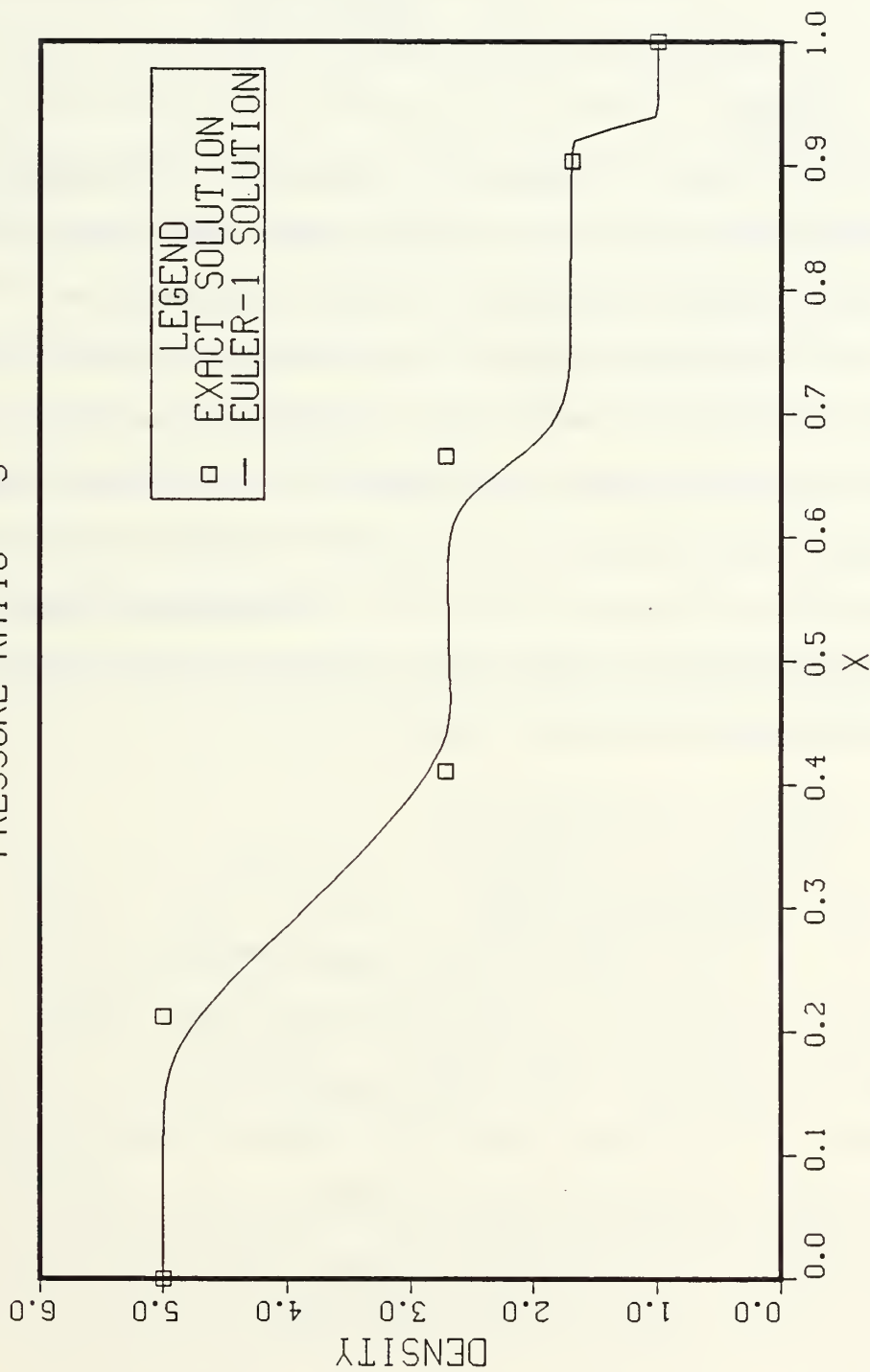


Figure 14. Exact Solution Comparison for Pressure Ratio 5, without Shock Tracking

V. DISCUSSION

A. RESULTS

The transient instability noted in the results was not investigated since the amplitude was small and the effect would be of no consequence in most applications.

At low pressure ratios, the velocity of propagation of the tail of the rarefaction wave approached sound speed and, in these cases, the EULER-1 code did not accurately compute its location. The reason for this was not investigated here; however, due to the low pressure ratios at which wave rotors can operate, this is of interest and should be investigated in future work.

B. SPECIAL CONSIDERATIONS

1. Modified Entropy

In the QAZ1D method, and subsequently, in the EULER-1 code, the variable S , which here has been referred to as the "modified entropy" and which is referred to in Reference 6 as simply the "entropy," does not behave thermodynamically as one would expect entropy to behave. As a fluid crosses a shock wave, the modified entropy of the fluid decreases. This is the result of the definition of Eq. (3), repeated here, that

$$dS = - \frac{1}{\gamma} \frac{dQ_R}{T}$$

The use of the word "entropy" and symbol "S" for this variable is confusing since the sign of the change in "S" is in direct conflict with well-established conventions in thermodynamics. For example, Corollary 6 to the 2nd Law of Thermodynamics [Ref. 8:p. 88] would have to be changed to read, "The 'modified entropy' of an isolated system decreases or in the limit remains constant." At a minimum perhaps, the symbol \bar{S} to denote the "modified (negative and scaled) entropy" would be helpful. In practice of course, the change in the conventionally defined entropy can be recovered from the change in the modified entropy, simply by multiplying by $(-\gamma)$.

2. Moretti's Methods

Incorporating Moretti's methods of handling discontinuities [Ref. 7] into the EULER-1 code required special care.

There is a fundamental difference in procedure in that the EULER-1 code is based on the high pressure side being on the left whereas Moretti's formulations are all based on the high pressure side being on the right. Although essentially a matter of bookkeeping, it is an area of potential confusion.

Another difference is that the Riemann variables used by Moretti are not the Riemann variables used in the QAZ1D method. This can lead to difficulty. In fact, in the application of Moretti's shock tracking scheme to the EULER-1 code, the pressures and densities have to be non-dimensionalized

by their values on the low pressure side of the shock in order to obtain Eq. (14), and for the procedure to work.

C. SUITABILITY FOR WAVE ROTOR APPLICATIONS

Further work is necessary before the suitability of the QAZ1D method for wave rotor applications can be fully evaluated. The following areas need to be addressed.

1. Boundary Conditions

In the EULER-1 code, boundary conditions at the ends of the passage have not been incorporated. The code calculates the changes of the interior nodes only, skipping the two end nodes. In particular, solid wall boundary conditions and open-end boundary conditions must be incorporated. No particular problems are expected in the boundary conditions themselves. However, additional logic may be necessary in the handling of discontinuities, such as the reversal of conditions to the left and right of a discontinuity after reflection from a boundary. The additional logic, which may be considerable, is warranted by the simplicity of the QAZ1D method.

2. Contact Discontinuity

No special attention is given to the contact discontinuity in the EULER-1 code and hence the discontinuity is smeared. In a wave rotor application, this discontinuity will have to be sharp. Moretti's methods again appear to be applicable here and the additional logic needs only to be formulated and incorporated into the EULER-1 code.

3. Quasi-One-Dimensional Modeling

EULER-1 is a one-dimensional code. The solution of flows in passages of varying area may be desirable for some wave rotor applications. Such problems can be solved in a quasi-one-dimensional manner by the addition of the appropriate area variation term to the equations, and the need to solve the fully two-dimensional equations is avoided. The area variation must be incorporated into the EULER-1 code and the code tested on quasi-one-dimensional problems.

4. Other Potential Extensions

Another capability which can be incorporated is the ability to handle two gases with different specific heat ratios. Eventually, the code should be extended also to a second order, one-dimensional version and then to a first order, two-dimensional version.

VI. CONCLUSIONS

The development of the EULER equations in the natural streamline coordinates using extended Riemann variables was reviewed in detail. The QAZ1D solution method, with the addition of shock tracking features, was implemented in a first order, one-dimensional FORTRAN code with the intent of evaluating the method's suitability for wave rotor applications. The code (EULER-1) was tested on the shock tube problem with good results. The incorporation of boundary conditions, an improvement in the contact discontinuity definition and the addition of an area variation term for quasi-one-dimensional modeling are considered to be necessary before the QAZ1D method can be accepted as being suitable for wave rotor applications. The additional logic required for these extensions may be considerable but the development is warranted by the overall simplicity of the QAZ1D method, and its straightforward extension to viscous, multi-dimensional flow modeling.

APPENDIX A

DERIVATION OF THE GOVERNING EQUATIONS FOR THREE-DIMENSIONAL INVISCID FLOW (WITH AREA CHANGE)

The governing equations of a 3-D, inviscid, compressible, unsteady flow are derived here in a natural streamline coordinate system. The equations are then recast along characteristic trajectories in the (s,t) plane and expressed in extended Riemann variables, reducing the system of partial differential equations to a system of ordinary differential equations.

A. DEFINITION OF VARIABLES

A	Cross-sectional area of a differential stream tube
A	Speed of sound
C_p	Specific heat at constant pressure
C_v	Specific heat at constant volume
$d\vec{a}$	Normal vector for differential area of control surface
e	Specific internal energy
$\hat{i}_{s,n,m}$	Unit vectors in the s , n , and m directions
P	Static pressure
Q	Modified Riemann variable
Q_R	Reversible heat transferred
q	Velocity magnitude
\vec{r}	Position vector

R	Modified Riemann variable
R_G	Gas constant
S	Modified entropy
T	Static temperature
t	Time
u	Velocity relative to a standing shock wave
v	Specific volume
vol	Differential element of volume
\bar{V}	Velocity vector
W	Incoming Mach number relative to a standing shock wave
ρ	Density
γ	Ratio of specific heats
θ, ϕ	Flow angles with respect to reference coordinate planes .
∇	Vector operator

B. THE COORDINATE SYSTEM

The natural streamline coordinate system (s,n,m) is shown with respect to a fixed rectangular cartesian system (x,y,z) in Fig. A1. The system is a curvilinearly translating, right hand orthogonal system which translates with a fluid particle along a streamline such that the 's' coordinate is measured in the direction of the flow. The 'n' coordinate direction always lies in the plane defined by the 's' coordinate direction and the fixed 'y' axis. The 'm' direction is normal to the (s,n) coordinate surface. The flow angles, θ and ϕ , are defined as shown in Fig. A1.

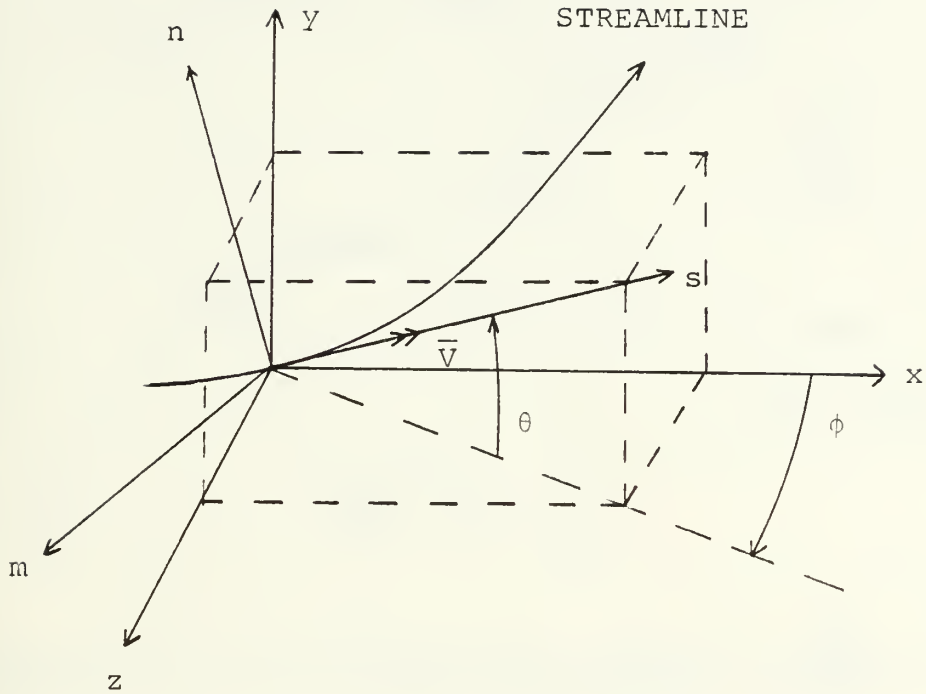


Figure A1. The Natural Coordinate System

C. VECTOR OPERATORS IN THE NATURAL COORDINATE SYSTEM

1. $\nabla()$

If $d\vec{r}$ is the position vector of a fluid particle

$$d\vec{r} \cdot \nabla() = d() \quad (A1)$$

In natural coordinates, Eq. (A1) becomes

$$\begin{aligned} [\hat{i}_s ds + \hat{i}_n dn + \hat{i}_m dm] \cdot [() \hat{i}_s + () \hat{i}_n + () \hat{i}_m] \\ = \frac{\partial ()}{\partial s} ds + \frac{\partial ()}{\partial n} dn + \frac{\partial ()}{\partial m} dm \end{aligned}$$

By inspection,

$$\nabla () = \frac{\partial ()}{\partial s} \hat{i}_s + \frac{\partial ()}{\partial n} \hat{i}_n + \frac{\partial ()}{\partial m} \hat{i}_m \quad (A2)$$

2. $\underline{\bar{V} \cdot \nabla ()}$

Since

$$\bar{V} = q \hat{i}_s$$

using Eq. (A2)

$$\bar{V} \cdot \nabla () = q \frac{\partial ()}{\partial s} \quad (A3)$$

3. $\underline{\nabla \cdot \bar{V}}$

From Eq. (A2) with $\bar{V} = q \hat{i}_s$

$$\nabla \cdot \bar{V} = \frac{\partial q}{\partial s} \quad (A4)$$

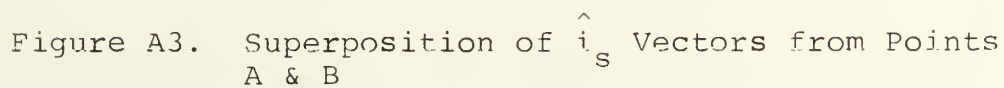
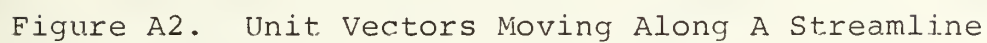
4. $\underline{(\bar{V} \cdot \nabla) \bar{V}}$

From Eq. (A3) with $\bar{V} = q \hat{i}_s$

$$(\bar{V} \cdot \nabla) \bar{V} = q \frac{\partial \bar{V}}{\partial s} = q \frac{\partial (q \hat{i}_s)}{\partial s} = q \left[\frac{\partial q}{\partial s} \hat{i}_s + q \frac{\partial \hat{i}_s}{\partial s} \right] \quad (A5)$$

The change in the unit vector \hat{i}_s with respect to s is derived below and is illustrated in Figs. A2 through A6. (A three-dimensional model is very helpful in visualizing the vector geometry.)

Figure A2 illustrates the natural coordinate system translating along a streamline from point A to point B in



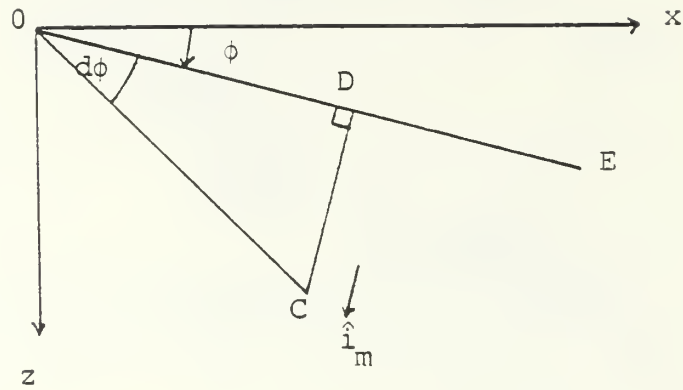


Figure A5. X-Z Plane

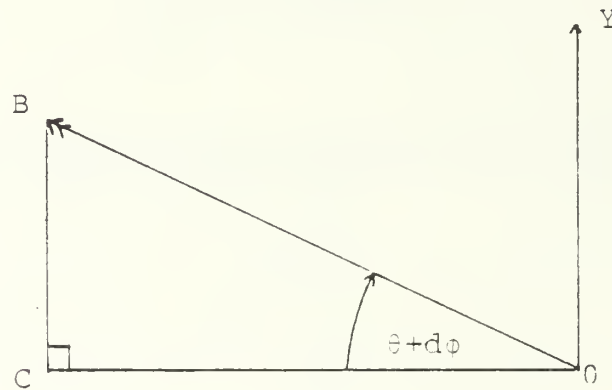


Figure A4. Plane Formed by B Vector and Y Axis

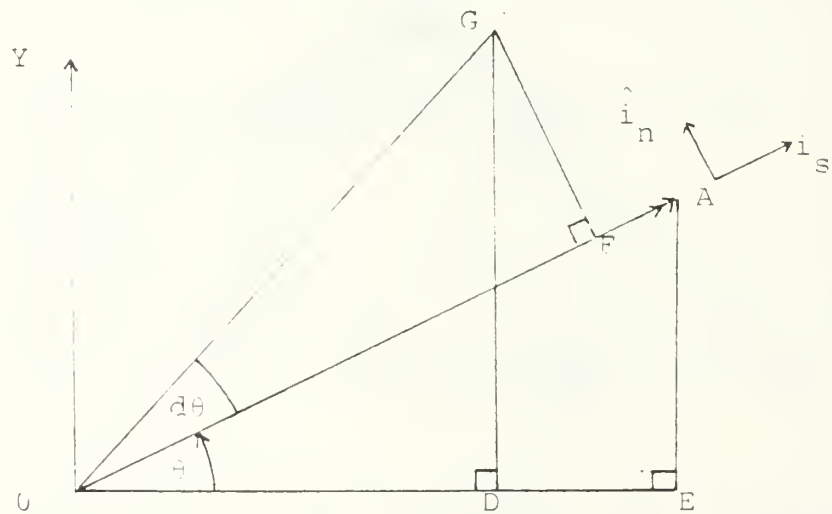


Figure A6. Plane Formed by A Vector and Y Axis

the inertial cartesian coordinate system. Figure A3 is the superposition of the \hat{i}_s unit vector from points A and B of Fig. A2. The intent here is to express the change in the unit vector \hat{i}_s in terms of components along the original (s,n,m) directions shown at point A in Fig. A3. Vector \overline{OA} in Fig. A3 is the original \hat{i}_s direction and vector \overline{OB} is $\hat{i}_s + \frac{\partial \hat{i}_s}{\partial s} ds$. Points C and E are the projection of points B and A in the (x,z) plane respectively. Point D is the projection of point C onto the line \overline{OE} .

Figure A4 is the plane formed by the \overline{OB} vector and the Y axis. The length of \overline{OB} is unity by definition. The length of \overline{BC} is $\sin(\theta+d\theta)$.

$$\sin(\theta+d\theta) = \sin \theta \cos d\theta + \cos \theta \sin d\theta$$

which, since $d\theta$ is a small angle, is

$$\sin(\theta+d\theta) = \sin \theta + \cos \theta d\theta \quad (A6)$$

The length of \overline{OC} is $\cos(\theta+d\theta)$.

$$\cos(\theta+d\theta) = \cos \theta \cos d\theta - \sin \theta \sin d\theta$$

which, since $d\theta$ is a small angle, is

$$\cos(\theta+d\theta) = \cos \theta - \sin \theta d\theta \quad (A7)$$

Figure A5 is the (x,z) plane in which the angle ϕ is defined. The \hat{i}_m direction is shown at point C. The length of \overline{CD} is $\overline{OC} \sin d\phi$ which, with Eq. (A7) is

$$[\cos \theta - \sin \theta d\theta] \sin d\phi$$

which, since $d\phi$ is a small angle, is

$$\cos \theta d\phi - \sin \theta d\theta d\phi$$

Dropping the second order term

$$\overline{CD} = \cos \theta d\phi \quad (A8)$$

The length of \overline{OD} is $\overline{OC} \cos d\phi$ which, since $d\phi$ is a small angle, is \overline{OC} .

Figure A6 is the plane formed by the \overline{OA} vector and the y axis. \overline{GD} is the projection of \overline{BC} and since both are vertical lines, \overline{BC} and \overline{GD} have the same length, which has been determined in Eq. (A6). The \hat{i}_s and \hat{i}_n directions are shown at point A. The lengths to be determined are \overline{AF} and \overline{GF} , since these are the components of \overline{AB} in the s and n directions. For small angles, \overline{OD} was shown to be equal to \overline{OC} and $\overline{GD} = \overline{BC}$, so that the angle GOD is equal to angle BOC = $\theta + d\theta$. Angle GOF is therefore $d\theta$, the length of \overline{OG} is unity and the length of \overline{GF} is $\sin d\theta$, which for small angles is $d\theta$, and it is in the \hat{i}_n direction. The length of \overline{AF} is $\overline{OA} - \overline{OF}$. \overline{OA} is unity

by definition and \overline{OF} is $\cos d\theta$, therefore \overline{AF} , the component of \overline{AB} in the \hat{i}_s direction is equal to $1 - \cos d\theta$, which, since $d\theta$ is a small angle, is zero.

The component of \overline{AB} in the \hat{i}_n direction is \overline{GF} or

$$d\theta \hat{i}_n \quad (A9)$$

The remaining component of \overline{AB} in the \hat{i}_m direction is \overline{CD} or

$$\cos \theta d\phi \hat{i}_m \quad (A10)$$

Therefore, the vector \overline{AB} can be written as

$$\begin{aligned} \frac{\partial \hat{i}_s}{\partial s} ds &= d\theta \hat{i}_n + \cos \theta d\phi \hat{i}_m \\ &= \frac{\partial \theta}{\partial s} ds \hat{i}_n + \cos \theta \frac{\partial \phi}{\partial s} ds \hat{i}_m \end{aligned}$$

and, dividing by ds , finally

$$\frac{\partial \hat{i}_s}{\partial s} = \frac{\partial \theta}{\partial s} \hat{i}_n + \cos \theta \frac{\partial \phi}{\partial s} \hat{i}_m \quad (A11)$$

Note that Fig. A3 can be considered also to describe a change in the unit vector \hat{i}_s at a fixed location, with respect to time. In this case, the vector \overline{AB} is equal to $\frac{\partial \hat{i}_s}{\partial t} dt$ and with Eq. (A9) and Eq. (A10)

$$\frac{\partial \hat{i}_s}{\partial t} = \frac{\partial \theta}{\partial t} \hat{i}_n + \cos \theta \frac{\partial \phi}{\partial t} \hat{i}_m \quad (A12)$$

With Eq. (A11), Eq. (A5) becomes

$$(\bar{V} \cdot \nabla) \bar{V} = q \frac{\partial q}{\partial s} \hat{i}_s + q^2 \frac{\partial \theta}{\partial s} \hat{i}_n + q^2 \cos \theta \frac{\partial \phi}{\partial s} \hat{i}_m \quad (A13)$$

D. CONSERVATION OF MASS

In the quasi-one-dimensional differential stream tube, shown in Figure A7, where \hat{i}_s is always in the direction of \bar{V} , ρ , q , and the cross sectional area A are known at the center of the element and ρ and q are assumed constant on any given cross section.

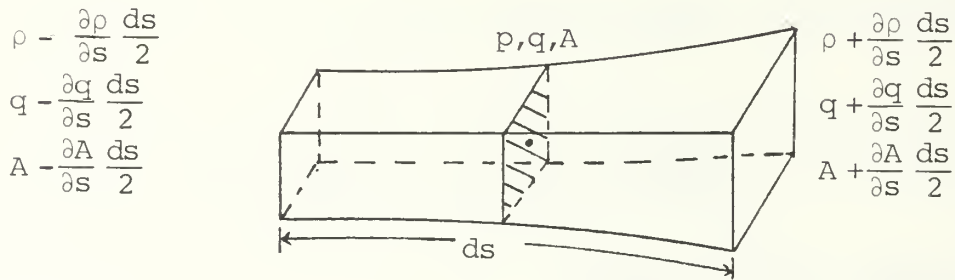


Figure A7. Differential Stream Tube of Variable Cross Section

The statement of continuity is

$$\left[\begin{array}{l} \text{The change in the mass} \\ \text{within the control volume} \\ \text{with respect to time} \end{array} \right] = \left[\begin{array}{l} \text{The net influx of} \\ \text{mass across the} \\ \text{control surface} \end{array} \right]$$

Since the volume is constant, the left side becomes

$$A \, ds \, \frac{\partial \rho}{\partial t}$$

For the stream tube, mass enters and leaves only from the ends so that the right hand side can be written as

$$[\rho - \frac{\partial \rho}{\partial s} \frac{ds}{2}] [q - \frac{\partial q}{\partial s} \frac{ds}{2}] [A - \frac{\partial A}{\partial s} \frac{ds}{2}] - [\rho + \frac{\partial \rho}{\partial s} \frac{ds}{2}] [q + \frac{\partial q}{\partial s} \frac{ds}{2}] [A + \frac{\partial A}{\partial s} \frac{ds}{2}]$$

which on expansion becomes

$$- \rho q \frac{\partial A}{\partial s} ds - qA \frac{\partial \rho}{\partial s} ds - \rho A \frac{\partial q}{\partial s} ds - \frac{\partial \rho}{\partial s} \frac{\partial q}{\partial s} \frac{\partial A}{\partial s} ds^3$$

On dropping the higher order terms and combining with the left hand side,

$$\frac{\partial \rho}{\partial t} + \rho q \frac{1}{A} \frac{\partial A}{\partial s} + q \frac{\partial \rho}{\partial s} + \rho \frac{\partial q}{\partial s} = 0 \quad (A14)$$

Equation (A14) is the form of the continuity equation which is required to model a flow as being one-dimensional with area change. In general, however, $\frac{1}{A} \frac{\partial A}{\partial s}$ must be expressed in terms of q , θ and ϕ .

With reference to Fig. A8, the change in the cross-sectional area of the stream tube can be written as

$$\frac{\partial A}{\partial s} ds = [dm + \frac{\partial dm}{\partial s} ds] [dn + \frac{\partial dn}{\partial s} ds] - A \quad (A15)$$

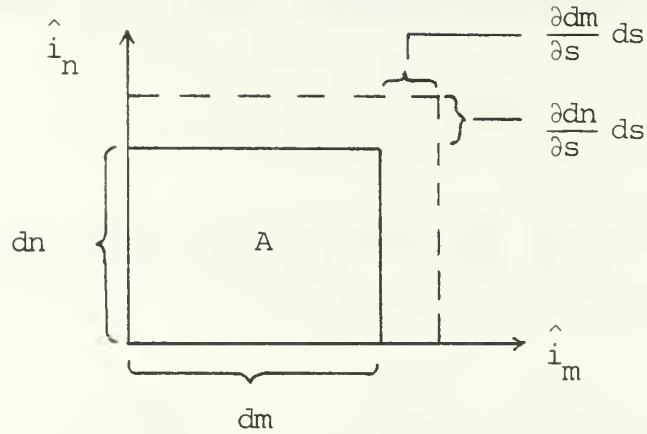


Figure A8. Cross Section of a Diverging Differential Stream Tube

After expansion, dividing by A and dropping the higher order terms, Eq. (A15) becomes

$$\frac{1}{A} \frac{\partial A}{\partial s} = \frac{1}{dn} \frac{\partial dn}{\partial s} + \frac{1}{dm} \frac{\partial dm}{\partial s} \quad (\text{A16})$$

From Fig. A9,

$$\frac{1}{dn} \frac{\partial dn}{\partial s} ds = \frac{1}{dn} \frac{ds}{\cos(\frac{\partial \theta}{\partial n} dn)} \sin(\frac{\partial \theta}{\partial n} dn)$$

which, for small angles, becomes

$$\frac{1}{dn} \frac{\partial dn}{\partial s} = \frac{\partial \theta}{\partial n} \quad (\text{A17})$$

From Fig. A10,

$$\frac{1}{dm} \frac{\partial dm}{\partial s} ds = \frac{1}{dm} \overline{AB} \quad (\text{A18})$$

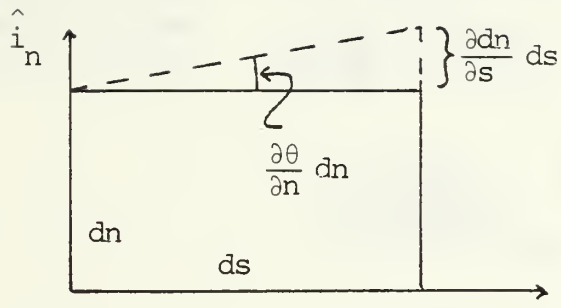


Figure A9. (s,n) Plane of Diverging Differential Stream Tube

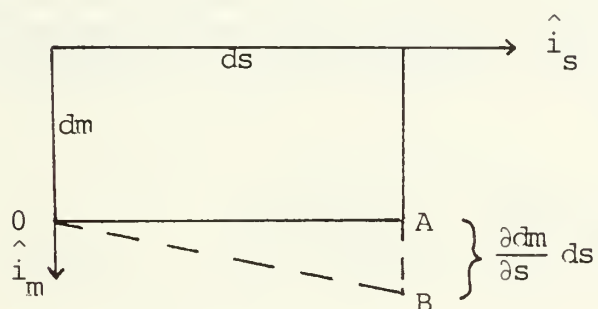


Figure A10. (s,m) Plane of Diverging Differential Stream Tube

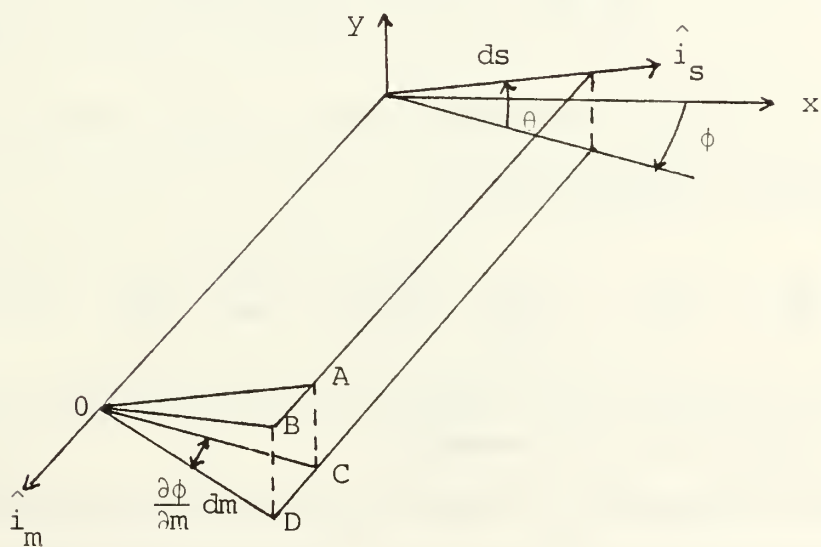


Figure A11. (s,m) Plane and its Projection onto the (x,z) Plane

With reference to Fig. A11, $\overline{AB} = \overline{CD}$, and

$$\overline{CD} = \overline{OD} \sin \left[\frac{\partial \phi}{\partial m} dm \right] \quad (A19)$$

$$\overline{OD} = \frac{\overline{OC}}{\cos \left[\frac{\partial \phi}{\partial m} dm \right]} \quad (A20)$$

$$\overline{OC} = ds \cos \theta \quad (A21)$$

Combining Eqs. (A18) through (A21) and knowing that $\frac{\partial \phi}{\partial m} dm$ is a small angle,

$$\frac{1}{dm} \frac{\partial dm}{\partial s} = \cos \theta \frac{\partial \phi}{\partial m} \quad (A22)$$

Equation (A16), with Eqs. (A17) and (A22), becomes

$$\frac{1}{A} \frac{\partial A}{\partial s} = \frac{\partial \theta}{\partial n} + \cos \theta \frac{\partial \phi}{\partial m} \quad (A23)$$

With Eq. (A23), the general form of the continuity equation in natural coordinates is

$$\frac{\partial \rho}{\partial t} + q \frac{\partial \rho}{\partial s} + \rho \frac{\partial q}{\partial s} + \rho q \left[\frac{\partial \theta}{\partial n} + \cos \theta \frac{\partial \phi}{\partial m} \right] = 0 \quad (A24)$$

E. CONSERVATION OF MOMENTUM

The statement of conservation for an arbitrary control volume which is fixed in the reference frame can be written as

$$\begin{aligned}
& \left[\begin{array}{l} \text{The change in the} \\ \text{momentum of the fluid} \\ \text{in the control volume} \\ \text{with respect to time} \end{array} \right] = \left[\begin{array}{l} \text{The net influx} \\ \text{of momentum} \\ \text{across the con-} \\ \text{trol surface} \end{array} \right] + \left[\begin{array}{l} \text{The net force} \\ \text{on the con-} \\ \text{trol surface} \end{array} \right] \\
& \quad + \left[\begin{array}{l} \text{The net} \\ \text{body} \\ \text{force} \\ \text{on the fluid} \end{array} \right]
\end{aligned}$$

Assuming the fluid is inviscid, the only forces acting on the control surface are pressure forces. In the absence of any body forces (gravity, electromagnetic, etc.), the statement becomes

$$\frac{\partial}{\partial t} \iiint \rho \bar{V} \, d\text{vol} = - \iint \bar{V} \rho \bar{V} \cdot d\vec{a} - \iint P \, d\vec{a} = 0 \quad (\text{A25})$$

With Gauss' Theorem, Eq. (A25) becomes

$$\iiint \frac{\partial}{\partial t} [\rho \bar{V}] \, d\text{vol} + \iiint \nabla \cdot [\bar{V} \rho \bar{V}] \, d\text{vol} + \iiint \nabla P \, d\text{vol} = 0$$

or

$$\iiint \left\{ \frac{\partial}{\partial t} [\rho \bar{V}] + \nabla \cdot [\bar{V} \rho \bar{V}] + \nabla P \right\} d\text{vol} = 0 \quad (\text{A26})$$

Since Eq. (A26) is true for any volume, the integrand must be zero, thus

$$\frac{\partial}{\partial t} [\rho \bar{V}] + \nabla \cdot [\bar{V} \rho \bar{V}] + \nabla P = 0 \quad (\text{A27})$$

Expanding the first term of Eq. (A27) and using the vector identity

$$\nabla \cdot [\bar{V} \rho \bar{V}] = \bar{V} [\nabla \cdot \rho \bar{V}] + \rho (\bar{V} \cdot \nabla) \bar{V}$$

Eq. (17) becomes

$$\rho \frac{\partial \bar{V}}{\partial t} + \bar{V} \left\{ \frac{\partial \rho}{\partial t} + \nabla \cdot \rho \bar{V} \right\} + \rho (\bar{V} \cdot \nabla) \bar{V} + \nabla P = 0 \quad (\text{A28})$$

The second term of Eq. (A28) is zero by the conservation of mass so that Eq. (A28) reduces to

$$\rho \frac{\partial \bar{V}}{\partial t} + \rho (\bar{V} \cdot \nabla) \bar{V} + \nabla P = 0 \quad (\text{A29})$$

Using Eqs. (A2), (A5), (A11) and (A12), collecting terms and equating each vector component to zero, Eq. (A29) becomes

$$\hat{i}_s \left[\rho \frac{\partial q}{\partial t} + \rho q \frac{\partial q}{\partial s} + \frac{\partial P}{\partial s} \right] = 0 \quad (\text{A30})$$

$$\hat{i}_n \left[\rho q \frac{\partial \theta}{\partial t} + \rho q^2 \frac{\partial \theta}{\partial s} + \frac{\partial P}{\partial n} \right] = 0 \quad (\text{A31})$$

$$\hat{i}_m \left[\rho q \cos \theta \frac{\partial \phi}{\partial t} + \rho q^2 \cos \theta \frac{\partial \phi}{\partial s} + \frac{\partial P}{\partial m} \right] = 0 \quad (\text{A32})$$

Using the perfect gas relation

$$A^2 = \frac{\gamma P}{\rho}$$

and the identity

$$\frac{\partial P}{\partial s} = P \frac{\partial \ln P}{\partial s}$$

Eqs. (A30) through (A32) become

$$\frac{\partial q}{\partial t} + q \frac{\partial q}{\partial s} = - \frac{A^2}{\gamma} \frac{\partial \ln P}{\partial s} \quad (\text{A33})$$

$$\frac{\partial \theta}{\partial t} + q \frac{\partial \theta}{\partial s} = - \frac{A^2}{\gamma q} \frac{\partial \ln P}{\partial n} \quad (\text{A34})$$

$$\frac{\partial \phi}{\partial t} + q \frac{\partial \phi}{\partial s} = - \frac{A^2}{\gamma q \cos \theta} \frac{\partial \ln P}{\partial m} \quad (\text{A35})$$

which are in the desired form.

F. CONSERVATION OF ENERGY

The conservation of energy for an arbitrary control volume is

$$\left[\begin{array}{l} \text{The rate of increase of} \\ \text{energy within the con-} \\ \text{trol volume with respect} \\ \text{to time} \end{array} \right] = \left[\begin{array}{l} \text{The rate at which energy} \\ \text{is entering the control} \\ \text{volume across the} \\ \text{boundary} \end{array} \right] + \left[\begin{array}{l} \text{The net rate of} \\ \text{work done on the} \\ \text{fluid at the} \\ \text{boundary} \end{array} \right] \quad (\text{A36})$$

Neglecting gravitational potential, the energy per unit mass is

$$e + \frac{q^2}{2}$$

where e is the internal energy per unit mass and q is the velocity magnitude. For an inviscid fluid in the absence of body forces, the only work done on the fluid is pressure work. Thus Eq. (A36) is written mathematically as

$$\frac{\partial}{\partial t} \iiint [e + \frac{q^2}{2}] \rho \, dvol = - \iiint [e + \frac{q^2}{2}] \rho \bar{V} \cdot d\vec{A} - \iint P \bar{V} \cdot d\vec{a} \quad (A37)$$

Using Gauss' Theorem, Eq. (A37) is written as

$$\begin{aligned} \iiint \frac{\partial}{\partial t} [e + \frac{q^2}{2}] \rho \, dvol &= - \iiint \nabla \cdot [(e + \frac{q^2}{2}) \rho \bar{V}] \, dvol \\ &- \iiint \nabla \cdot [P \bar{V}] \, dvol \end{aligned}$$

or

$$\frac{\partial \rho}{\partial t} [e + \frac{q^2}{2}] + \nabla \cdot [(e + \frac{q^2}{2}) \rho \bar{V}] = - \nabla \cdot [P \bar{V}]$$

Expanding,

$$\begin{aligned} \frac{\partial \rho}{\partial t} [e + \frac{q^2}{2}] + \rho \frac{\partial}{\partial t} [e + \frac{q^2}{2}] + (\rho \bar{V}) \cdot \nabla [e + \frac{q^2}{2}] + [e + \frac{q^2}{2}] [\nabla \cdot (\rho \bar{V})] \\ = - \nabla \cdot [P \bar{V}] \end{aligned}$$

or

$$\begin{aligned}
\left[e + \frac{q^2}{2}\right] \left[\frac{\partial \rho}{\partial t} + \nabla \cdot (\rho \bar{V})\right] + \rho \frac{\partial}{\partial t} \left[e + \frac{q^2}{2}\right] + (\rho \bar{V}) \nabla \cdot \left[e + \frac{q^2}{2}\right] \\
= -\nabla \cdot [P \bar{V}]
\end{aligned} \tag{A38}$$

The first term of Eq. (A38) is zero according to the conservation of mass. Expanding the remaining terms of Eq. (A38),

$$\rho \frac{\partial}{\partial t} \left[e + \frac{q^2}{2}\right] + \rho q \frac{\partial}{\partial x} \left[e + \frac{q^2}{2}\right] = -\nabla \cdot [P \bar{V}]$$

or

$$\frac{D}{Dt} \left[e + \frac{q^2}{2}\right] = -\frac{1}{\rho} \nabla \cdot [P \bar{V}] \tag{A39}$$

Equation (A39) can be written as

$$\frac{De}{Dt} + \frac{D}{Dt} \left[\frac{q^2}{2}\right] = -\frac{1}{\rho} (\bar{V} \cdot \nabla P) - \frac{P}{\rho} (\nabla \cdot \bar{V}) \tag{A40}$$

With $\bar{V} = \hat{q} i_s$ in the natural coordinate system, Eq. (A29) becomes

$$\frac{\partial \bar{V}}{\partial t} + q \frac{\partial \bar{V}}{\partial s} = -\frac{1}{\rho} \nabla P$$

or

$$\frac{D \bar{V}}{Dt} = -\frac{1}{\rho} \nabla P \tag{A41}$$

Taking the dot product of \bar{V} with Eq. (A41),

$$\bar{V} \cdot \frac{D\bar{V}}{Dt} = - \frac{1}{\rho} [\bar{V} \cdot \nabla P] \quad (A42)$$

and substituting Eq. (A42) into Eq. (A40)

$$\frac{De}{Dt} + \frac{D}{Dt} \left[\frac{q^2}{2} \right] = \bar{V} \cdot \frac{D\bar{V}}{Dt} - \frac{P}{\rho} (\nabla \cdot \bar{V}) \quad (A43)$$

But

$$\begin{aligned} \frac{D\bar{V}}{Dt} &= \frac{D(q\hat{i}_s)}{Dt} = \frac{Dq}{Dt} \hat{i}_s + q \frac{D\hat{i}_s}{Dt} \\ &= \frac{Dq}{Dt} \hat{i}_s + q \left[\frac{\partial \hat{i}_s}{\partial t} + q \frac{\partial \hat{i}_s}{\partial s} \right] \end{aligned}$$

and using Eq. (A11) and Eq. (A12),

$$\begin{aligned} \frac{D\bar{V}}{Dt} &= \frac{Dq}{Dt} \hat{i}_s + q \left[\frac{\partial \theta}{\partial t} \hat{i}_n + \cos \theta \frac{\partial \phi}{\partial t} \hat{i}_m \right] \\ &\quad + q^2 \left[\frac{\partial \theta}{\partial s} \hat{i}_n + \cos \theta \frac{\partial \phi}{\partial s} \hat{i}_m \right] \end{aligned}$$

Therefore

$$\begin{aligned} \bar{V} \cdot \frac{D\bar{V}}{Dt} &= q\hat{i}_s \cdot \left\{ \frac{Dq}{Dt} \hat{i}_s + \left[q \frac{\partial \theta}{\partial t} + q^2 \frac{\partial \theta}{\partial s} \right] \hat{i}_n + q \cos \theta \left[\frac{\partial \phi}{\partial t} + q \frac{\partial \phi}{\partial s} \right] \hat{i}_m \right\} \\ &= q \frac{Dq}{Dt} = \frac{D}{Dt} \left[\frac{q^2}{2} \right] \end{aligned}$$

Therefore Eq. (A43) reduces to

$$\frac{De}{Dt} = - \frac{P}{\rho} (\nabla \cdot \bar{V}) \quad (A44)$$

From the conservation of mass

$$\frac{\partial \rho}{\partial t} + \nabla \cdot (\rho \bar{V}) = 0$$

or

$$\frac{\partial \rho}{\partial t} + \bar{V} \cdot \nabla \rho + \rho (\nabla \cdot \bar{V}) = 0$$

which, in the natural coordinate system gives,

$$\frac{\partial \rho}{\partial t} + q \frac{\partial \rho}{\partial s} = -\rho (\nabla \cdot \bar{V})$$

or

$$- \frac{1}{\rho} \frac{D\rho}{Dt} = (\nabla \cdot \bar{V}) \quad (A45)$$

Substituting Eq. (10) into Eq. (9),

$$\frac{De}{Dt} - \frac{P}{2} \frac{D\rho}{Dt} = 0 \quad (A46)$$

The definition of the modified entropy is

$$dS = - \frac{1}{\gamma} \frac{dQ_R}{T}$$

and the first law of thermodynamics for an elemental mass requires that

$$dQ_R = de + Pd\left(\frac{1}{\rho}\right)$$

so that

$$\begin{aligned} dS &= -\frac{1}{\gamma T} [de + Pd\left(\frac{1}{\rho}\right)] \\ &= -\frac{1}{\gamma T} [de + \frac{P}{2} d\rho] \end{aligned}$$

and Eq. (A46) implies that

$$\frac{DS}{Dt} = 0 \quad (A47)$$

which states that modified entropy is conserved along streamlines

G. MODIFIED ENTROPY EVALUATION

With the modified entropy defined as

$$dS = -\frac{dQ_R}{\gamma T}$$

or

$$S_B - S_A = -\frac{1}{\gamma} \int_A^B \frac{dQ_R}{T} \quad (A48)$$

From the first law of thermodynamics

$$dQ_R = de + P dv \quad (A49)$$

where e is the internal energy and v is the specific volume.

Substituting Eq. (A49) into Eq. (A48),

$$S_A - S_B = \frac{1}{\gamma} \int_A^B \frac{de + P dv}{T} = \frac{1}{\gamma} \left[\int_A^B \frac{de}{T} + \int_A^B \frac{P dv}{T} \right] \quad (A50)$$

For a perfect gas

$$P v = R_G T \quad \text{and} \quad de = C_v dT$$

for which Eq. (A50) becomes

$$S_A - S_B = \frac{1}{\gamma} \left[\int_A^B \frac{C_v dT}{T} + \int_A^B \frac{R_G dv}{v} \right]$$

which after integration yields

$$S_A = S_B + \frac{1}{\gamma} \left[C_v \ln \frac{T_B}{T_A} + R \ln \frac{v_B}{v_A} \right] \quad (A51)$$

Substituting

$$R_G = C_v (\gamma - 1)$$

into Eq. (A51)

$$S_A = S_B + \frac{1}{\gamma} [C_V (\ln \frac{T_B}{T_A} - \ln \frac{v_B}{v_A}) + C_V \gamma \ln \frac{v_B}{v_A}]$$

$$S_A = S_B + \frac{1}{\gamma} [\frac{R_G}{\gamma-1} \ln (\frac{P_B v_B R_A v_A}{P_A v_A R_B v_B}) + \frac{\gamma R}{\gamma-1} \ln \frac{\rho_A}{\rho_B}]$$

and since $R_{G_A} = R_{G_B}$

$$S_A = S_B + \frac{R}{\gamma(\gamma-1)} [\ln \frac{P_B}{P_A} - \gamma \ln \frac{\rho_B}{\rho_A}]$$

or

$$\frac{S_A}{R_G} = \frac{S_B}{R_G} + \frac{1}{\gamma(\gamma-1)} [\ln \frac{P_B}{\rho_B^\gamma} - \ln \frac{P_A}{\rho_A^\gamma}]$$

or

$$\frac{S_B}{R_G} = \frac{S_A}{R_G} + \frac{1}{\gamma(\gamma-1)} [\ln \frac{P_A}{\rho_A^\gamma} - \ln \frac{P_B}{\rho_B^\gamma}] \quad (A52)$$

If the reference condition is chosen to be

$$\frac{S_A}{R_G} = \frac{2}{\gamma-1} - \frac{1}{\gamma(\gamma-1)} \ln \frac{P_A}{\rho_A^\gamma}$$

Eq. (A52) becomes

$$\frac{S_B}{R_G} = \frac{2}{\gamma-1} - \frac{1}{\gamma(\gamma-1)} \ln \frac{P_B}{\rho_B^\gamma} \quad (A53)$$

H. FURTHER TRANSFORMATIONS

Equations (A24), (A33) through (A35) and (A47) are in the required form. However, some of the variables need to be transformed, namely, derivatives of $\ln P$ need to be expressed in terms of A and S and derivatives of ρ must be expressed in terms of q and A .

Using the first law of thermodynamics expressed as

$$dQ = dh - \frac{1}{\rho} dP$$

Eq. (A48) may be written as

$$-\gamma T \nabla S = \nabla h - \frac{1}{\rho} \nabla P$$

or for the \hat{i}_S component

$$-\gamma \frac{\partial S}{\partial s} = \frac{1}{T} \frac{\partial C_p^T}{\partial s} - \frac{P}{\rho T} \frac{\partial \ln P}{\partial s} \quad (A54)$$

Assuming C_p to be constant and using the equation of state for a perfect gas Eq. (A54) becomes

$$-\gamma \frac{\partial S}{\partial s} = \frac{C_p}{T} \frac{\partial}{\partial s} \left[\frac{P}{R_G \rho} \right] - R \frac{\partial \ln P}{\partial s}$$

and since $C_p = \gamma R / (\gamma - 1)$

$$-\gamma \frac{\partial S}{\partial s} = \frac{\gamma R_G}{(\gamma - 1)} \frac{\rho R_G}{P} \frac{\partial}{\partial s} \left[\frac{P}{R_G \rho} \right] - R_G \frac{\partial \ln P}{\partial s}$$

Since R is a constant it may be moved in or out of the derivatives giving

$$- \gamma \frac{\partial}{\partial s} \left[\frac{S}{R_G} \right] = \frac{\gamma}{\gamma-1} \frac{\rho}{P} \frac{\partial}{\partial s} \left[\frac{P}{\rho} \right] - \frac{\partial \ln P}{\partial s}$$

and since γ is also constant, similarly

$$- \gamma \frac{\partial}{\partial s} \left[\frac{S}{R_G} \right] = \frac{\gamma}{\gamma-1} \frac{\rho}{P\gamma} \frac{\partial}{\partial s} \left[\frac{P\gamma}{\rho} \right] - \frac{\partial \ln P}{\partial s}$$

Using $A^2 = \gamma P / \rho$

$$\begin{aligned} - \gamma \frac{\partial}{\partial s} \left[\frac{S}{R_G} \right] &= \frac{\gamma}{\gamma-1} \frac{1}{A^2} \frac{\partial A^2}{\partial s} - \frac{\partial \ln P}{\partial s} \\ &= \frac{2A\gamma}{(\gamma-1)A^2} \frac{\partial A}{\partial s} - \frac{\partial \ln P}{\partial s} \end{aligned}$$

and, on rearranging

$$\frac{\partial \ln P}{\partial s} = \frac{2\gamma}{\gamma-1} \frac{1}{A} \frac{\partial A}{\partial s} + \gamma \frac{\partial}{\partial s} \left[\frac{S}{R} \right] \quad (\text{A55})$$

Substituting Eq. (A55) into Eq. (A33) yields

$$\frac{\partial q}{\partial t} + q \frac{\partial q}{\partial s} + \frac{2A}{\gamma-1} \frac{\partial A}{\partial s} + A^2 \frac{\partial}{\partial s} \left[\frac{S}{R} \right] = 0 \quad (\text{A56})$$

and the derivative of $\ln P$ has been removed.

Since

$$A^2 = \frac{\gamma P}{\rho}$$

logarithmic differentiation yields

$$2 \frac{dA}{A} = \frac{dP}{P} + \frac{d\gamma}{\gamma} - \frac{d\rho}{\rho} \quad (A57)$$

For a pure substance

$$P = P(\rho, S)$$

and an isentropic process

$$P = P(\rho)_S$$

Differentiating

$$\left(\frac{\partial P}{\partial \rho}\right)_S = \frac{dP}{d\rho} = \frac{\gamma P}{\rho} = A^2$$

therefore

$$\frac{dP}{P} = \gamma \frac{d\rho}{\rho} \quad (A58)$$

Substituting Eq. (A58) into Eq. (A57) gives

$$2 \frac{dA}{A} = \gamma \frac{d\rho}{\rho} - \frac{d\rho}{\rho} = \gamma^{-1} \frac{d\rho}{\rho}$$

or

$$d\rho = \frac{2\rho}{(\gamma-1)} \frac{dA}{A} \quad (\text{A59})$$

Along a streamline

$$d\rho = \frac{\partial \rho}{\partial t} + q \frac{\partial \rho}{\partial s} \quad (\text{A60})$$

and since the fluid is the same from streamline to streamline Eqs. (A59) and Eq. (A60) can be combined giving

$$\frac{\partial \rho}{\partial t} + q \frac{\partial \rho}{\partial s} = \frac{2\rho}{\gamma-1} \frac{dA}{A} = \frac{2\rho}{(\gamma-1)A} \left[\frac{\partial A}{\partial t} + q \frac{\partial A}{\partial s} \right] \quad (\text{A61})$$

Substituting Eq. (A61) into Eq. (A24) yields

$$\frac{\partial A}{\partial t} + q \frac{\partial A}{\partial s} + \frac{\gamma-1}{2} A \frac{\partial q}{\partial s} + q A \frac{\gamma-1}{2} \left[\frac{\partial \theta}{\partial n} + \cos \theta \frac{\partial \phi}{\partial m} \right] = 0 \quad (\text{A62})$$

and the derivatives of ρ have been removed.

The governing equations are now summarized:

$$\frac{\partial A}{\partial t} + q \frac{\partial A}{\partial s} + \frac{\gamma-1}{2} A \frac{\partial q}{\partial s} + q A \frac{\gamma-1}{2} \left[\frac{\partial \theta}{\partial n} + \cos \theta \frac{\partial \phi}{\partial m} \right] = 0 \quad (\text{A63})$$

$$\frac{\partial q}{\partial t} + q \frac{\partial q}{\partial s} + \frac{2A}{\gamma-1} \frac{\partial A}{\partial s} + A^2 \frac{\partial}{\partial s} \left[\frac{S}{R} \right] = 0 \quad (\text{A64})$$

$$\frac{\partial \theta}{\partial t} + q \frac{\partial \theta}{\partial s} = - \frac{A^2}{\gamma q} \frac{\partial \ln P}{\partial n} \quad (\text{A65})$$

$$\frac{\partial \phi}{\partial t} + q \frac{\partial \phi}{\partial s} = - \frac{A^2}{\gamma q \cos \theta} \frac{\partial \ln P}{\partial m} \quad (\text{A66})$$

$$\frac{\partial S}{\partial t} + q \frac{\partial S}{\partial s} = 0 \quad (\text{A67})$$

Note that Eqs. (A65) through (A67) are in the form

$$\frac{\partial X}{\partial t} + \lambda \frac{\partial X}{\partial s} = z$$

If $X = X(s, t)$, then

$$dX = \frac{\partial X}{\partial t} dt + \frac{\partial X}{\partial s} ds$$

and

$$\frac{dX}{dt} = \frac{\partial X}{\partial t} + \frac{ds}{dt} \frac{\partial X}{\partial s} \quad (\text{A68})$$

where (ds/dt) is the "characteristic" direction in the (s, t) plane along which Eq. (A68) holds. Along this direction, the equations may be transformed from partial to ordinary differential equations. What is desirable is to find transformed variables in terms of which Eqs. (A63) and (A64) will be in the same characteristic form. For this reason the modified Riemann variables

$$Q = q + AS/R_G \quad (\text{A69})$$

$$R = q - AS/R_G \quad (\text{A70})$$

are defined, where S/R_G is defined in Eq. (A53). The modified Riemann variables can be introduced by manipulation of the equations as follows. First, multiplying Eq. (A63) by S , gives

$$S \frac{\partial A}{\partial t} + q S \frac{\partial A}{\partial s} + \frac{\gamma-1}{2} A S \frac{\partial q}{\partial s} + q A S \frac{\gamma-1}{2} \left[\frac{\partial \theta}{\partial n} + \cos \theta \frac{\partial \phi}{\partial m} \right] = 0 \quad (A71)$$

and multiplying Eq. (A67) by A gives

$$A \frac{\partial S}{\partial t} + q A \frac{\partial S}{\partial s} = 0 \quad (A72)$$

On adding Eqs. (A71) and (A72) to Eq. (A64), and introducing

$$A \frac{\partial q}{\partial t} - A \frac{\partial q}{\partial s} = 0 \quad (A73)$$

and

$$A S \frac{\partial A}{\partial s} - A S \frac{\partial A}{\partial s} = 0 \quad (A74)$$

after appropriate rearrangement

$$\begin{aligned} \frac{\partial q}{\partial t} + A \frac{\partial S}{\partial t} + S \frac{\partial A}{\partial t} + q \frac{\partial q}{\partial s} + q A \frac{\partial S}{\partial s} + q S \frac{\partial A}{\partial s} + A \frac{\partial q}{\partial s} \\ + A^2 \frac{\partial S}{\partial s} + A S \frac{\partial A}{\partial s} = - \frac{\gamma-1}{2} A S \frac{\partial q}{\partial s} + A S \frac{\partial A}{\partial s} + A \frac{\partial q}{\partial s} \\ - \frac{2A}{\gamma-1} \frac{\partial A}{\partial s} - \frac{\gamma-1}{2} q A S \left[\frac{\partial \theta}{\partial n} + \cos \theta \frac{\partial \phi}{\partial m} \right] = 0 \end{aligned}$$

Rearranging and introducing Eq. (A69) gives

$$\begin{aligned} \frac{\partial Q}{\partial t} + (q+A) \frac{\partial Q}{\partial s} &= - \frac{\gamma-1}{2} A \left[S - \frac{2}{\gamma-1} \right] \left[\frac{\partial}{\partial s} \left(q - \frac{2}{\gamma-1} A \right) \right] \\ &\quad - \frac{\gamma-1}{2} q A S \left[\frac{\partial \theta}{\partial n} + \cos \theta \frac{\partial \phi}{\partial m} \right] \end{aligned} \quad (A75)$$

By subtracting Eqs. (A71) and (A72) from Eq. (A64), again using Eq. (A73) and Eq. (A74), and introducing Eq. (A70), one also obtains

$$\begin{aligned} \frac{\partial R}{\partial t} + (q-A) \frac{\partial R}{\partial s} &= \frac{\gamma-1}{2} A \left[S - \frac{2}{\gamma-1} \right] \left[\frac{\partial}{\partial s} \left(q + \frac{2}{\gamma-1} A \right) \right] \\ &\quad + \frac{\gamma-1}{2} q A S \left[\frac{\partial \theta}{\partial n} + \cos \theta \frac{\partial \phi}{\partial m} \right] \end{aligned} \quad (A76)$$

Together with Eqs. (A65) through (A67), Eqs. (A75) and (A76) form the system of equations which describe the isentropic flow of an inviscid perfect gas under unsteady, compressible conditions, and which may be solved as a system of ordinary differential equations along characteristic trajectories in the space-time domain.

I. SHOCK JUMP EQUATION

The analytical expression for the change in the extended Riemann variable, Q , across a stationary shock is derived below.

Consider a shock moving with a velocity V_s into a fluid with velocity q_B as depicted in Fig. A12, with the conditions

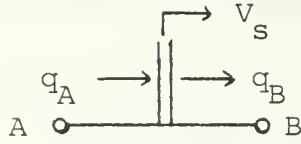


Figure A12

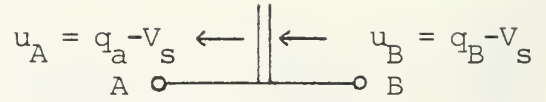


Figure A13

to the left of the shock being denoted by A subscripts and conditions to the right by B subscripts. If a velocity of $-V_s$ is imposed on the entire system, the situation becomes one of a stationary shock, as depicted in Fig. A13. In both cases, the high pressure side is to the left (A side). Since all velocities are defined positive to the right, a positive value for the relative mach number is defined as

$$W = - \frac{u_B}{A_B} = - \frac{(q_B - V_s)}{A_B} \quad (\text{A77})$$

The extended Riemann variable, Q , is defined as

$$Q \equiv q + AS \quad (\text{A78})$$

where

$$S \equiv \frac{2}{\gamma-1} - \frac{1}{\gamma(\gamma-1)} \ln \left[\frac{p}{\rho^\gamma} \right] \quad (\text{A79})$$

If all velocities are non-dimensionalized by A_B and pressures and densities are non-dimensionalized by their values at B,

$$\frac{Q_A - Q_B}{A_B} = \left[\frac{q_A + A_A S_A}{A_B} \right] - \left[\frac{q_B + A_B S_B}{A_B} \right]$$

$$\frac{Q_A - Q_B}{A_B} = \frac{q_A - q_B}{A_B} + \frac{A_A}{A_B} S_A - S_B$$

$$= \frac{q_A - q_B}{A_B} + \frac{A_A}{A_B} \left[\frac{2}{\gamma-1} - \frac{1}{\gamma(\gamma-1)} \ln \frac{p_A}{p_B} \left(\frac{\rho_A}{\rho_B} \right)^\gamma \right]$$

$$- \left[\frac{2}{\gamma-1} - \frac{1}{\gamma(\gamma-1)} \ln \frac{p_B}{p_A} \left(\frac{\rho_B}{\rho_A} \right)^\gamma \right]$$

$$= \frac{q_A - q_B}{A_B} + \left[\frac{A_A}{A_B} - 1 \right] \frac{2}{\gamma-1} - \left(\frac{A_A}{A_B} \right) \frac{1}{\gamma(\gamma-1)} \left[\ln \frac{p_A}{p_B} \left(\frac{\rho_B}{\rho_A} \right)^\gamma \right]$$

(A80)

The ratios of pressure, density and sound speed across a normal shock are well known functions of γ and the Mach number which in this case is W . They are

$$\frac{p_A}{p_B} = \frac{2\gamma}{\gamma+1} W^2 - \frac{\gamma-1}{\gamma+1} \quad (A81)$$

$$\frac{\rho_A}{\rho_B} = \frac{(\gamma+1) W^2}{(\gamma-1) W^2 + 2} \quad (A82)$$

$$\frac{A_A}{A_B} = \frac{1}{(\gamma+1) W} \left\{ 2(\gamma-1) \left[1 + \frac{\gamma-1}{2} W^2 \right] \left[\frac{2\gamma}{\gamma-1} W^2 - 1 \right] \right\}^{1/2} \quad (A83)$$

An expression for $(q_A - q_B)/A_B$ is obtained using mass conservation.

$$\rho_A u_A = \rho_B u_B$$

$$\frac{u_A}{u_B} = \frac{\rho_B}{\rho_A} = \frac{(\gamma-1)W^2 + 2}{(\gamma+1)W^2}$$

Subtracting one from both sides,

$$\frac{u_A - u_B}{u_B} = \frac{(\gamma-1)W^2 + 2 - (\gamma+1)W^2}{(\gamma+1)W^2}$$

$$\frac{u_A - u_B}{u_B} = \frac{2(1 - W^2)}{(\gamma+1)W^2} \quad (\text{A84})$$

Substituting Eq. (A77) for u_B in Eq. (A84) gives

$$\frac{u_A - u_B}{-W^A_B} = \frac{2(1 - W^2)}{(\gamma+1)W^2}$$

$$\frac{u_A - u_B}{A_B} = \frac{2(W^2 - 1)}{(\gamma+1)W} \quad (\text{A85})$$

Since $u_A = q_A - v_s$ and $u_B = q_B - v_s$

$$u_A - u_B = q_A - v_s - q_B + v_s = q_A - q_B$$

Thus Eq. (A85) can be written as

$$\frac{q_A - q_B}{A_B} = \frac{2(W^2 - 1)}{(\gamma + 1)W} \quad (\text{A86})$$

Substituting Eqs. (A86) and (A81) through (A83) into Eq. (A80) gives

$$\begin{aligned} \frac{Q_A - Q_B}{A_B} &= \frac{2(W^2 - 1)}{(\gamma + 1)W} + \frac{2}{\gamma - 1} \left\{ \frac{1}{(\gamma + 1)W} [2(\gamma - 1) \left(1 + \frac{\gamma - 1}{2} W^2\right) \left(\frac{2\gamma}{\gamma - 1} W^2 - 1\right)]^{1/2} \right. \\ &\quad \left. - 1 \right\} - \left\{ \frac{1}{(\gamma + 1)W} [2(\gamma - 1) \left(1 + \frac{\gamma - 1}{2} W^2\right) \left(\frac{2\gamma}{\gamma - 1} W^2 - 1\right)]^{1/2} \right\} \\ &\quad \times \left\{ \frac{1}{\gamma(\gamma - 1)} \left[\ln \left(\frac{2\gamma}{\gamma + 1} W^2 - \frac{\gamma - 1}{\gamma + 1} \right) \left(\frac{(\gamma - 1)W^2 + 2}{(\gamma + 1)W^2} \right)^\gamma \right] \right\} \quad (\text{A87}) \end{aligned}$$

APPENDIX B
USING EULER-1 ON THE NPS VM/CMS SYSTEM

A. MEMORY REQUIREMENTS

Storage should be defined as one mega-byte to ensure adequate memory for DISSPLA requirements. Also ensure that room exists on the user's disk for the listing file if that output option is selected.

B. TERMINAL REQUIREMENTS

The type of terminal required to run EULER-1 depends on the output option selected. When using the tabular listing output, any terminal tied into the VM/CMS system may be used. Graphical output may also be created using any terminal and the graph stored on the user's disk in a metafile for later viewing at a graphics terminal or for printing. To have the graph stored on the disk, use the "COMPRS" command on line 223 of the program and comment out the "TEK618" command on line 224. When graphical output is selected and it is desired to view the graph at the terminal at execution time, an IBM 3277-Tek618 dual screen terminal must be used. To use this option, use the "TEK618" command on line 224 and comment out the "COMPRS" command on line 223. When using this option, a low quality hard copy of the TEK618 display may be obtained using the TEK4631 hard copy unit attached.

C. PROCEDURE AND COMMANDS

After logging on to VM/CMS, use the command "DEFINE STORAGE 1M" to increase the virtual memory as recommended above. This will remove you from the CMS environment. Re-enter CMS with the command "I CMS."

Edit the user input area of EULER-1 FORTRAN as desired for the particular problem being run. When graphical output is selected, comment out either the "COMPRS" or the "TEK618" command as desired.

Compute the program using the command "FORTVS EULER-1." After compilation, an EULER-1 TEXT and an EULER-1 LISTING file will reside on the user's disk. At execution, if a tabular output has been selected, it will be sent to the user's disk as "FILE FT09F001." To give this file a particular name, say "EULER-1 LISTING," use the file definition command

```
"F I 9 DISK EULER-1 LISTING A ( PERM"
```

at compile time. An alternate and convenient means of compiling the program is to set up an exec file on the user's disk by the name "EULER-1 EXEC" which contains the commands

```
F I 9 DISK EULER-1 LISTING A ( PERM  
FORTVS EULER-1
```

Then to compile the program and define the output file, use the command "EULER-1."

After compilation, to execute the program, use the command "DISPLA EULER-1." The message

...YOUR FORTRAN PROGRAM IS NOW BEING LOADED...

...EXECUTION WILL SOON FOLLOW...

should appear, followed shortly by

...EXECUTION BEGINS...

If tabular output was selected, proper termination will result in a ready message. If graphical output was selected using the TEK618 option, the plot will appear on the TEK618 terminal, the program will pause, and a

"...press ENTER to continue"

message will be displayed on the 3277 terminal. At this point the hard copy must be made, if desired, using the TEK4631 hard copy unit. After pressing the ENTER key on the 3277 terminal, the plot will be erased and the program will terminate. Proper termination will be indicated by the message

"END OF DISSPLAY 9.2 #### VECTORS IN 1 PLOT..."

and a ready message.

EULER-1 FORTRAN CODE

EUL00010
EUL00020
EUL00030
EUL00040
EUL00050
EUL00060
EUL00070
EUL00080
EUL00090
EUL00100
EUL00110
EUL00120
EUL00130
EUL00140
EUL00150
EUL00160
EUL00170
EUL00180
EUL00190
EUL00200
EUL00210
EUL00220
EUL00230
EUL00240
EUL00250
EUL00260
EUL00270
EUL00280
EUL00290
EUL00300
EUL00310
EUL00320
EUL00330
EUL00340
EUL00350
EUL00360
EUL00370
EUL00380
EUL00390
EUL00400
EUL00410
EUL00420
EUL00430
EUL00440
EUL00450
EUL00460
EUL00470
EUL00480

EUL000490
EUL000500
EUL000510
EUL000520
EUL000530
EUL000540
EUL000550
EUL000560
EUL000570
EUL000580
EUL000590
EUL000600
EUL000610
EUL000620
EUL000630
EUL000640
EUL000650
EUL000660
EUL000670
EUL000680
EUL000690
EUL000700
EUL000710
EUL000720
EUL000730
EUL000740
EUL000750
EUL000760
EUL000770
EUL000780
EUL000790
EUL000800
EUL000810
EUL000820
EUL000830
EUL000840
EUL000850
EUL000860
EUL000870
EUL000880
EUL000890
EUL000900
EUL000910
EUL000920
EUL000930
EUL000940
EUL000950
EUL000960

L - DENOTES WHICH TYPE OF DISCONTINUITY IS
BEING DEALT WITH:
1 = SHOCK 2 = CONTACT DISCONTINUITY
3 = HEAD OF EXPANSION WAVE
4 = TAIL OF EXPANSION WAVE

----- VARIABLE DEFINITIONS -----

A - SPEED OF SOUND
CUNT - COUNTER FOR GRAPHICS ROUTINES
DARRAY - ARRAY OF DENSITY FOR PLOTTING
DELT - TIME STEP
DLCD - DENSITY TO THE LEFT OF THE CONTACT
DISCONTINUITY IN THE EXACT SOLUTION.
DLSH - DENSITY TO THE LEFT OF THE SHOCK IN THE
EXACT SOLUTION.
DRI - INITIAL DENSITY RATIO ACROSS THE SHOCK
EE - DESIRED PRECISION FOR CHARACTERISTIC CALCULATIONS
G - GAMMA (RATIO OF SPECIFIC HEATS)
GRAPHS - FOR GRAPHICAL OUTPUT, 0=NONE (TABULAR)
1=PLOTS ALL VARIABLES
2=COMPARES DENSITY WITH EXACT SOLUTION
G1 - $1/(G-1)$
G2 - $2/(G-1)$
H - $1/(N-1)$
I2 - NODE # UPSTREAM OF A DISCONTINUITY
JSTOP - NUMBER OF TIME LEVELS TO BE CALCULATED
M - A NUMBER WHICH INDICATES WHICH
DISCONTINUITIES WILL BE TREATED:
1 - SHOCK ONLY
2 - SHOCK AND CONTACT DISCONTINUITY
3 - NUMBER OF SPACIAL NODES (ODD NUMBER)
ND - DOUBLE PRECISION VALUE OF N
PAKRAY - ARRAY OF PRESSURES FOR PLOTTING
PRI - INITIAL PRESSURE RATIO ACROSS THE SHOCK
PLTCNT - COUNTER FOR GRAPHICS ROUTINES
Q - ABSOLUTE FLUID VELOCITY
QARRAY - ARRAY OF VELOCITIES FOR PLOTTING
QLI - INITIAL VELOCITY LEFT OF THE DIAPHRAGM
QRI - INITIAL VELOCITY RIGHT OF THE DIAPHRAGM
QW - Q+A*S (EXTENDED RIEMANN VARIABLE)
RR - Q-A*S (EXTENDED RIEMANN VARIABLE)
S - ENTROPY
SARRAY - ARRAY OF ENTROPY FOR PLOTTING
SIGMA - SPATIAL LOCATION OF DISCONTINUITIES
SIGMA(L,J) WHERE L INDICATES THE TYPE OF
DISCONTINUITY AND J INDICATES THE
TIME LEVEL; 1 - CURRENT LEVEL

CC

```

2 - LEVEL BEING CALCULATED
- VARIABLE WHICH INDICATES HOW MANY TIME
- TIME SINCE INITIAL CONDITIONS
- INITIAL TEMP. RATIO ACROSS THE SHOCK
- VELOCITY OF THE HEAD OF THE EXPANSION
WAVE FOR THE EXACT SOLUTION.
VTAIL - VELOCITY OF THE TAIL OF THE EXPANSION
WAVE FOR THE EXACT SOLUTION.
VCDE - VELOCITY OF THE CONTACT DISCONTINUITY
FOR THE EXACT SOLUTION.
VSE - VELOCITY OF THE SHOCK FOR THE EXACT
SOLUTION.
W - MACH NO. RELATIVE TO A STANDING SHOCK
XARRAY - ARRAY OF SPATIAL POSITIONS FOR PLOTTING
XEXACT - ARRAY OF SIX X VALUES FOR THE EXACT SOLUTION.
XINIT - INITIAL POSITION OF DISCONTINUITY FOR
EXACT SOLUTION PLOTTING.
X2 - LOCATION OF NOISE UPSTREAM OF DISCONT.
ALONG THE SPACIAL AXIS.
Y - (N+1)/2
YEXACT - ARRAY OF SIX DENSITY VALUES FOR THE EXACT SOLUTION.

*** OTHER VARIABLES ARE DEFINED IN THE
SUBROUTINES WHERE THEY ARE USED ***

+++++ PROBLEM SET - UP
+
+
+
+++++

THE PARTICULAR PROBLEM FOR THIS VERSION IS:

SHOCK TUBE, SINGLE CENTERED DIAPHRAGM WITH
HIGH PRESSURE SIDE TO THE LEFT.

BOUNDARY CONDITIONS - NONE (INFINITE LENGTH)

----- VARIABLE DECLARATIONS -----
INTEGER I,J,K,L,N,JSTOP,Y,M,GRAPHS,COUNT,PLTCNT
INTEGER SKIP
REAL#8 TRI,PRI,QLI,QRI,DR I,G,G1,G2,SIGMA(4,2),EE
REAL#8 DELT,H,ND,I2(4),X2(4),AR,W,DQ,VS,T
REAL VTAIL,VCDE,VSE,DLSH,DLCD,XINIT,VHEAD
REAL XEXACT(6),YEXACT(6)

```

EUL00970
EUL00980
EUL00990
EUL01000
EUL01010
EUL01020
EUL01030
EUL01040
EUL01050
EUL01060
EUL01070
EUL01080
EUL01090
EUL01100
EUL01110
EUL01120
EUL01130
EUL01140
EUL01150
EUL01160
EUL01170
EUL01180
EUL01190
EUL01200
EUL01210
EUL01220
EUL01230
EUL01240
EUL01250
EUL01260
EUL01270
EUL01280
EUL01290
EUL01300
EUL01310
EUL01320
EUL01330
EUL01340
EUL01350
EUL01360
EUL01370
EUL01380
EUL01390
EUL01400
EUL01410
EUL01420
EUL01430
EUL01440

C

```

C C C
+++++++ USER INPUT REQUIRED HERE ++++++++
----- SET THE DIMENSIONS EQUAL TO N.-----
REAL*8 A(51),Q(51),QQ(51),RR(51),S(51)
REAL*8 NEWRR(51),NEWS(51),NEWQQ(51)
REAL PARRAY(51),DARRAY(51),SARRAY(51)
REAL QARRAY(51),XARRAY(51)
C C
----- ENTER THE APPROPRIATE VALUES BELOW -----
N=51
M=1
GRAPHS=2
SKIP=24
JSTGP=26
TRI=1.0D00
PRI=5.0D00
DRI=5.0D00
GLI=0.0D00
QRI=0.0D00
G=1.4D00
C C
----- EXACT SOLUTION VALUES -----
XINIT=0.5
VHEAD=-1.0
VTAIL=-0.310557
VCDE=.574487
VSE=1.402346
DLCD=2.713115
DLSH=1.69344
C C C
+++++++ END OF USER INPUT AREA ++++++++
SIGMA(1,2)=0.50000001D00
SIGMA(2,2)=0.50000001D00
SIGMA(3,2)=0.50000001D00
SIGMA(4,2)=0.50000001D00
EE=0.1D-8
T=0.0D00
DO 10 I=1,4
  I2(I)=0.0D00
  X2(I)=0.0D00
  SIGMA(I,1)=0.0D00
10 CONTINUE
ND=N
H=1/(ND-1)
DC 11 I=1,N
  A(I)=0.0D00
  Q(I)=0.0D00
EJL01450
EJL01460
EJL01470
EJL01480
EJL01490
EJL01500
EJL01510
EJL01520
EJL01530
EJL01540
EJL01550
EJL01560
EJL01570
EJL01580
EJL01590
EJL01600
EJL01610
EJL01620
EJL01630
EJL01640
EJL01650
EJL01660
EJL01670
EJL01680
EJL01690
EJL01700
EJL01710
EJL01720
EJL01730
EJL01740
EJL01750
EJL01760
EJL01770
EJL01780
EJL01790
EJL01800
EJL01810
EJL01820
EJL01830
EJL01840
EJL01850
EJL01860
EJL01870
EJL01880
EJL01890
EJL01900
EJL01910
EJL01920

```


EUL01930
 EUL01940
 EUL01950
 EUL01960
 EUL01970
 EUL01980
 EUL01990
 EUL02000
 EUL02010
 EUL02020
 EUL02030
 EUL02040
 EUL02050
 EUL02060
 EUL02070
 EUL02080
 EUL02090
 EUL02100
 EUL02110
 EUL02120
 EUL02130
 EUL02140
 EUL02150
 EUL02160
 EUL02170
 EUL02180
 EUL02190
 EUL02200
 EUL02210
 EUL02220
 EUL02230
 EUL02240
 EUL02250
 EUL02260
 EUL02270
 EUL02280
 EUL02290
 EUL02300
 EUL02310
 EUL02320
 EUL02330
 EUL02340
 EUL02350
 EUL02360
 EUL02370
 EUL02380
 EUL02390
 EUL02400

```

NEWQQ(I)=0.0D00
NEWRR(I)=0.0D00
NEWS(I)=0.0D00
QARRAY(I)=0.0
PARRAY(I)=0.0
DARRAY(I)=0.0
SARRAY(I)=0.0
XARRAY(I)=(I-1)*S NGL(H)
11 CONTINUE
DELT=2.0D00
Y=(N+1)/2
AR=1.0D00
DQ=0.0D00
W=1.0D00
VS=0.0D00
G1=1/(G-1)
G2=2/(G-1)
DO 12 I=1, Y
  S(I)=G2-(G1/G)*DLG(PRI/((DRI)**G))
  QQ(I)=QLI+DSQRT(TRI)*S(I)
  RR(I)=QLI-DSQRT(TRI)*S(I)
12 CONTINUE
Y=(N+3)/2
DO 13 I=Y, N
  S(I)=G2
  QQ(I)=QRI+S(I)
  RR(I)=QRI-S(I)
13 CONTINUE
C
IF (GRAPHS.GT.0) THEN
  CALL COMPRS
  CALL TEK618
  CALL HWROT('AUTO')
  CALL HWSCAL('SCREEN')
  IF (GRAPHS.EQ.2) THEN
    CALL PAGE(11.0,8.5)
  ELSE
    CALL PAGE(8.5,11.0)
  END IF
  IF (GRAPHS.EQ.1) THEN
    CALL BORDER(JSTOP)
  END IF
END IF
J=1
COUNT=1
IF (GRAPHS.EQ.1) THEN
  CALL PLOT(J,JSTOP,N,QQ,RR,S,H,XARRAY,PARRAY,
#DARRAY,QARRAY,SARRAY,G,G1,G2)

```


[illegible]


```

300 W=5.513294D00-DSQRT(3.0396408D01-((QQJ1+2.7574D00)/0.286337D00))
    DQ=2*(W*W-1)/(W*(G+1))
    AR=DSQRT(2*(G-1)*(1+((G-1)*W*W/2))*(G*G2*W*W-1))/((G+1)*W)
    PR=(2*G/(G+1))*W*W-((G-1)/(G+1))
    DR=((G-1)*W*W+2)/((G+1)*W*W)
    QQJE=DQ+(AR-1)*G2-(AR*G1/G)*DLOG(PR*(DR**G))
    WRITE(9,*) W,QQJE,QQJ0
    IF (DABS(QQJE-QQJ0).LT.0.1D-5) GOTO 310
    QQJ1=(QQJ0-QQJE)+QQJ1
    GOTO 300
310 VS=(QQB+RRB)+W*AB
    TS=H/VS
311 IF (TS.LT.DELT) THEN
    DELT=0.99D00*TS
    END IF
    SIGMA(1,2)=VS*DELT+SIGMA(1,1)
    RETURN
    END
SUBROUTINE SWEEP(N,H,SIGMA,QQ,RR,S,DELT,EE,Q,A,NEWQQ,NEWRR,NEWS,
#12,G2,J)
*****
*      SPACE SWEEPING SUBROUTINE      *
*****
----- VARIABLE DEFINITIONS -----
DELQQH - CHANGE IN QQ FROM I TO I+1
DELQQL - CHANGE IN QQ FROM I-1 TO I
DELRHH - CHANGE IN RR FROM I TO I+1
DELRRL - CHANGE IN RR FROM I-1 TO I
DELSH - CHANGE IN S FROM I TO I+1
DELSL - CHANGE IN S FROM I-1 TO I
DELAH - CHANGE IN A FROM I TO I+1
DELAH - CHANGE IN A FROM I-1 TO I
DELQH - CHANGE IN Q FROM I TO I+1
DELQL - CHANGE IN Q FROM I-1 TO I
DELX - INTERPOLATION DISTANCE (LMD*DELT)
DLTA** - PREFIX WHICH INDICATES THE SPATIAL
          CHANGE IN ** FOR ONE TIME STEP.
E(K) - ACTUAL ERROR IN CHARACTERISTIC SLOPE CALCULATION.
INTEG(K) - RESULT OF INTEGRATING Z(K).
LMD - SLOPE OF THE CHARACTERISTICS (Q+A,Q-Q-A)
NEW***(I) - STORED VALUES OF ** FOR THE NEXT TIME LVL
*PRIM(K) - SUFFIX WHICH INDICATES THE SPATIAL

```

```

C C C C C C C
C      - DERIVATIVE OF * AT THE CURRENT TIME LEVEL.
C      - VALUE OF ** INTERPOLATED BETWEEN NODES
C      - ON THE CURRENT TIME LEVEL.
C      - THE CHANGE IN TIME OF ** AT A NODE
C      - USED TO STEP UP TO THE NEXT TIME LEVEL
C      - LOCATION IN SPACIAL PLANE (I-1)*H
C      - RIGHT SIDE OF THE K,TH EQUATION.
C
C      INTEGER N,K,I,I2(4),J
C      REAL*8 X,H,SIGMA(4,2),QQ(N),RR(N),S(N),Q(N),A(N)
C      REAL*8 DELQQH,DELQQL,DELRRL,DELSH,DELSL
C      REAL*8 DELAH,DELAL,DELQH,DELQL,LMD(3),DELDX(3),DELT
C      REAL*8 QINT(3),AINT(3),QINT,RKINT,SINT,EE,E(3)
C      REAL*8 NEWQQ(N),NEWRR(N),NEWS(N),QQSTEP
C      REAL*8 RRSTEP,SSTEP,INTEG(3),Z(3),DLTAQQ
C      REAL*8 DLTARR,DLTAS,APRIM(3),QPRIM(3)
C      DO 40 I=1,N
C      REAL*8 G2,ABAR(3)
C      Q(I)=(QQ(I)+RR(I))/2.0D00
C      A(I)=((QQ(I)-RR(I))/(2*S(I)))
C      40 CCNT INUE
C      I=2
C      41 IF (I.EQ.N) GOTO 49
C      X=(I-1)*H
C      DELQQH=QQ(I+1)-QQ(I)
C      DELQQL=QQ(I)-QQ(I-1)
C      DELRRH=RR(I+1)-RR(I)
C      DELRRL=RR(I)-RR(I-1)
C      DELSH=S(I+1)-S(I)
C      DELSL=S(I)-S(I-1)
C      DELAH=A(I+1)-A(I)
C      DELAL=A(I)-A(I-1)
C      DELQH=Q(I+1)-Q(I)
C      DELQL=Q(I)-Q(I-1)
C
C      ----- TEST FOR EXISTENCE OF A DISCONTINUITY
C
C      IF ((SIGMA(1,1).GT.X-H).AND.(SIGMA(1,1).LT.X)) THEN
C      IF (SIGMA(1,2).GT.X) THEN
C      QQSTEP=0.0D00
C      RRSTEP=0.0D00
C      SSTEP=0.0D00
C      GOTO 48
C      END IF
C      CALL LSHOCK(Q,A,RR,QQ,S,N,DELQQH,DELRRL,DELSH,DELAH
C      #,DELQH,H,EE,I,DELT,AINT,QQINT,RRINT,SINT)
C      GOTO 47
C      END IF
C
C C C

```



```

C
      IF ((SIGMA(1,1).GT.X).AND.(SIGMA(1,1).LT.X+H)).AND.
      # (Q(I).LE.A(I)) THEN
      CALL RSHOCK(Q,A,RR,QQ,S,N,DELQQL,DELRRL,DELSL,DELQL,DELAL
      #,H,EE,I,DELT,AINT,QQINT,RRINT,SINT)
      GOTO 47
      END IF

      LMD(1)=QQ(I-1)+A(I-1)
      LMD(2)=Q(I)
      IF (Q(I).LT.A(I)) GOTO 42
      LMD(3)=Q(I)-A(I)
      GOTO 43
      LMD(3)=Q(I+1)-A(I+1)
      K=1
      IF (K.EQ.4) GOTO 51
      DELX(K)=DELT*LMD(K)
      IF (LMD(K).GT.0.0D00) GOTO 44
      IF (LMD(K).LT.0.0D00) GOTO 45
      QINT(K)=Q(I)
      AINT(K)=A(I)
      GOTO 46
      QINT(K)=Q(I)-DELX(K)*DELQL/H
      AINT(K)=A(I)-DELX(K)*DELAL/H
      GOTO 46
      QINT(K)=Q(I)-DELX(K)*DELQH/H
      AINT(K)=A(I)-DELX(K)*DELAH/H
      K=K+1
      GOTO 50
      CONTINUE

      E(1)=DABS(LMD(1)-(QINT(1)+AINT(1)))
      E(2)=DABS(LMD(2)-QINT(2))
      E(3)=DABS(LMD(3)-(QINT(3)-AINT(3)))
      LMD(1)=QINT(1)+AINT(1)
      LMD(2)=QINT(2)
      LMD(3)=QINT(3)-AINT(3)
      IF ((E(1).GT.EE).OR.(E(2).GT.EE).OR.(E(3).GT.EE)) GOTO 43

      END OF ITERATION FOR LMD(K) & DELX(K) FOR THIS NODE

C
C
      QQINT=QQ(I)-DELX(1)*DELQQL/H
      IF (LMD(2).LE.0.0D00) THEN
      SINT=S(I)-DELX(2)*DELSL/H
      ELSE
      SINT=S(I)-DELX(2)*DELQL/H
      END IF
      IF (LMD(3).LE.0.0D00) THEN
EUL05290
EUL05300
EUL05310
EUL05320
EUL05330
EUL05340
EUL05350
EUL05360
EUL05370
EUL05380
EUL05390
EUL05400
EUL05410
EUL05420
EUL05430
EUL05440
EUL05450
EUL05460
EUL05470
EUL05480
EUL05490
EUL05500
EUL05510
EUL05520
EUL05530
EUL05540
EUL05550
EUL05560
EUL05570
EUL05580
EUL05590
EUL05600
EUL05610
EUL05620
EUL05630
EUL05640
EUL05650
EUL05660
EUL05670
EUL05680
EUL05690
EUL05700
EUL05710
EUL05720
EUL05730
EUL05740
EUL05750
EUL05760

```



```

C      IF ((E(1).GT.EE).OR.(E(2).GT.EE).OR.(E(3).GT.EE)) GOTO 420
C      QQINT=QQ(1)-DELX(1)*DELQQL/H
C      RRINT=RR(1)-DELX(3)*DELRRL/H
C      SINT=S(1)-DELX(2)*DELSL/H
C      RETURN
C      END
C      SUBROUTINE JUMP(N,SIGMA,H,QQ,RR,S,G,GI,M,I2,X2,W,AR,DQ,VS,J)
C      *****
C      * DISCONTINUITY CORRECTION SUBROUTINE *
C      * *****
C      *****
C      U - THE VELOCITY RELATIVE TO THE STEADY SHOCK WAVE.
C      INTEGER N,M,I,Y,L,I2(4),J
C      REAL*8 SIGMA(4,2),H,QQ(N),RR(N),S(N),X,XA(4)
C      REAL*8 XB(4),AB,SA,SB,QQA,QQB,RAA,RRB,W,DQ,AR,G
C      REAL*8 GI,VS,QA,QB,AA,UA,UB,SAI,SA2,X2(4)
C      ++++++++ LOCATING THE UPSTREAM NODE ++++++++
C      DO 62 L=1,M
C      Y=0
C      X=H
C      I=2
C      IF (.NOT.(Y.EQ.0)) GOTO 62
C      IF (SIGMA(L,2).LE.X) THEN
C      X2(L)=X
C      I2(L)=I
C      Y=1
C      END IF
C      X=X+H
C      I=I+1
C      GOTO 60
C      CONTINUE
C      +++++ CORRECTING THE VALUES AT NODE "A" +++++
C      IF ((SIGMA(1,2).GT.X2(1)-H).AND.(SIGMA(1,1).LT.X2(1)-H)) THEN
C      XA(1)=(SIGMA(1,2)+H-X2(1))/H
C      XB(1)=(X2(1)-SIGMA(1,2))/H
C      RRB=RR(I2(1))-XB(1)*(RR(I2(1))+1)-RR(I2(1))
C      QQB=QQ(I2(1))-XB(1)*(QQ(I2(1))+1)-Q(I2(1))
C      SB=S(I2(1))-XB(1)*(S(I2(1))+1)-S(I2(1))

```



```

C C
CALL HEADIN('PRESSURE RATIO = 5$',100,1.0,4)
CALL GRAF(0,'SCALE',1.0,0,'SCALE',JSTOP)
CALL ENDGR(0)
RETURN
END
EUL08170
EUL08180
EUL08190
EUL08200
EUL08210
EUL08220
EUL08230
EUL08240
EUL08250
EUL08260
EUL08270
EUL08280
EUL08290
EUL08300
EUL08310
EUL08320
EUL08330
EUL08340
EUL08350
EUL08360
EUL08370
EUL08380
EUL08390
EUL08400
EUL08410
EUL08420
EUL08430
EUL08440
EUL08450
EUL08460
EUL08470
EUL08480
EUL08490
EUL08500
EUL08510
EUL08520
EUL08530
EUL08540
EUL08550
EUL08560
EUL08570
EUL08580
EUL08590
EUL08600
EUL08610
EUL08620
EUL08630
EUL08640

C C
SUBROUTINE PLOT(J,JSTOP,N,QQ,RR,S,H,XARRAY,
#PARRAY,DARKAY,QARRAY,SAKRAY,G,G1,G2)
EUL08170
EUL08180
EUL08190
EUL08200
EUL08210
EUL08220
EUL08230
EUL08240
EUL08250
EUL08260
EUL08270
EUL08280
EUL08290
EUL08300
EUL08310
EUL08320
EUL08330
EUL08340
EUL08350
EUL08360
EUL08370
EUL08380
EUL08390
EUL08400
EUL08410
EUL08420
EUL08430
EUL08440
EUL08450
EUL08460
EUL08470
EUL08480
EUL08490
EUL08500
EUL08510
EUL08520
EUL08530
EUL08540
EUL08550
EUL08560
EUL08570
EUL08580
EUL08590
EUL08600
EUL08610
EUL08620
EUL08630
EUL08640

*****
*
* GRAPHICAL PLOTTING ROUTINE
*
*****
INTEGER I,N,J,JSTOP,KNT(4)/1,4,6,9/
REAL*8 QQ(N),RR(N),S(N),H,G,G1,G2
REAL XARRAY(N),QARRAY(N),PARRAY(N),DARRAY(N)
REAL SARRAY(N),TEMP
REAL XORG(4)/1.75,4.65,1.75,4.65/
REAL YORG(4)/2.75,2.75,5.80,5.80/
REAL YMAX(4)/5.5,5.5,1.5,6.20/
REAL YMIN(4)/0.5,0.5,-0.5,4.90/
CHARACTER*4 IYNAM
DIMENSION IYNAM(13)
DATA IYNAM/'PRES','SURE','$','MODI','FIED','ENT','ROPY','$'/'
#ITY$, 'VELO', 'CITY', '$', 'MODI', 'FIED', 'ENT', 'ROPY', '$'
G=SNGL(G)
G1=SNGL(G1)
G2=SNGL(G2)
H=SNGL(H)
DO 85 I=1,N
  QQ(I)=SNGL(QQ(I))
  RR(I)=SNGL(RR(I))
  S(I)=SNGL(S(I))
CONTINUE
DO 80 I=1,N
  QARRAY(I)=(QQ(I)+RR(I))/2.0
  TEMP=(QQ(I)-RR(I))*((QQ(I)-RR(I))/(4*S(I)*S(I))
  DARRAY(I)=((1/TEMP)*EXP(G*(1-G)*(S(I)-G2)))*(-G1)
  SAKRAY(I)=S(I)
  PARRAY(I)=TEMP*DARKAY(I)
CONTINUE
DO 83 I=1,4
  CALL PHYSOR(XORG(I),YORG(I))
  CALL AREA2(2.4,2.4)
  CALL XNAME('X',1)
EUL08170
EUL08180
EUL08190
EUL08200
EUL08210
EUL08220
EUL08230
EUL08240
EUL08250
EUL08260
EUL08270
EUL08280
EUL08290
EUL08300
EUL08310
EUL08320
EUL08330
EUL08340
EUL08350
EUL08360
EUL08370
EUL08380
EUL08390
EUL08400
EUL08410
EUL08420
EUL08430
EUL08440
EUL08450
EUL08460
EUL08470
EUL08480
EUL08490
EUL08500
EUL08510
EUL08520
EUL08530
EUL08540
EUL08550
EUL08560
EUL08570
EUL08580
EUL08590
EUL08600
EUL08610
EUL08620
EUL08630
EUL08640

```



```

      CALL YNAME(IYNAM(KNT(I)),100)
      CALL GRAF(0.,SCALE,1.0,YMIN(I),SCALE,YMAX(I))
      IF (I.EQ.1) CALL CURVE(XARRAY,PARRAY,N,0)
      IF (I.EQ.2) CALL CURVE(XARRAY,DARRAY,N,0)
      IF (I.EQ.3) CALL CURVE(XARRAY,QARRAY,N,0)
      IF (I.EQ.4) CALL CURVE(XARRAY,SARRAY,N,0)
      CALL ENDGR(0)
83  CONTINUE
      RETURN
      END
      SUBROUTINE EXACT(N,XINIT,I,VHEAD,VTAIL,VCDE,VSE,DLCD,DLSH,QQ,RR,S,
      #H,XARRAY,DARRAY,G,G1,G2,DRI)
      *****
      *      EXACT SOLUTION COMPARISON ROUTINE      *
      *      *****
      *****
      INTEGER N
      REAL#8 QQ(N),RR(N),S(N),H,G,G1,G2,T,DRI
      REAL XEXACT(6),YEXACT(6),XINIT,VHEAD,VTAIL,VCDE
      REAL VSE,DLCD,DLSH,TEMP,XARRAY(N),DARRAY(N)
      XEXACT(1)=0.0
      XEXACT(2)=XINIT+T*VHEAD
      XEXACT(3)=XINIT+T*VTAIL
      XEXACT(4)=XINIT+T*VCDE
      XEXACT(5)=XINIT+T*VSE
      XEXACT(6)=1.0
      YEXACT(1)=SNGL(DRI)
      YEXACT(2)=YEXACT(1)
      YEXACT(3)=DLCD
      YEXACT(4)=YEXACT(3)
      YEXACT(5)=DLSH
      YEXACT(6)=1.0
      DO 90 I=1,N
      QQ(I)=SNGL(QQ(I))
      RR(I)=SNGL(RR(I))
      S(I)=SNGL(S(I))
      TEMP=(QQ(I)-RR(I))*(QQ(I)-RR(I))/(4*S(I)*S(I))
      DARRAY(I)=(1/TEMP)*EXP(G*(1-3)*(S(I)-G2))*(-G1)
      CONTINUE
      CALL PHYSOK(2.65,2.25)
      CALL NOBRDR
      CALL AKEA2D(6.75,4.0)
90

```

```

CALL XNAME('X',1)
CALL YNAME('DENSITY',7)
CALL HEADIN('DENSITY DISTRIBUTION$',100,1.3,4)
CALL HEADIN('FIRST ORDER' N = 51$,100,1.0,4)
CALL HEADIN('DENSITY RATIO = 5 TEMP RATIO = 1$',100,1.0,4)
CALL HEADIN('PRESSURE RATIO = 5$',100,1.0,4)
CALL LINES('EULER-1 SOLUTION$',IPKRAY,2)
CALL LINES('EXACT SOLUTION$',IPKRAY,1)
CALL FRAME(0.0,'SCALE',1.0,0.0,'SCALE',6.0)
CALL GRAF(0.0,'SCALE',1.0,0.0,'SCALE',6.0)
CALL MARKER(0)
CALL CURVE(XEXACT,YEXACT,6,-1)
CALL LEGLIN
CALL CJRVE(XARRAY,DARRAY,N,0)
CALL LEGEND(IPKRAY,2,4.25,2.75)
CALL LENDGR(0)
RETURN
END

```

```

EUL09133
EUL09140
EUL09150
EUL09160
EUL09170
EUL09180
EUL09190
EUL09200
EUL09210
EUL09220
EUL09230
EUL09240
EUL09250
EUL09260
EUL09270
EUL09280
EUL09290
EUL09300

```

LIST OF REFERENCES

1. Eidelman, S., Colella, P. and Shreeve, R.P., "Application of the Godunov Method and Higher Order Extensions of the Godunov Method to Cascade Flow Modeling," AIAA Journal, Vol. 22, No. 11, pp. 1609-1615, November, 1984.
2. Eidelman, S. and Shreeve, R.P., "Numerical Modeling of the Non-steady Thrust Produced by Intermittent Pressure Rise in a Diverging Channel," ASME Winter Annual Meeting, New Orleans, ASME Bk. No. G00273, December, 1984.
3. Eidelman, S., "The Problem of Gradual Opening in Wave Rotor Passages," AIAA Journal of Propulsion and Power, Vol. 1, No. 1, Jan-Feb., 1985.
4. Naval Postgraduate School Contractor Report NPS67-84-007CR, Development and Evolution of a Numerical Solution of the Euler Equations Using the Godunov Method, by S. Eidelman, November, 1984.
5. Naval Postgraduate School Contractor Report NPS67-85-006CR, Wave Rotor Research: A Computer Code for Preliminary Design of Wave Diagrams, by A. Mathur, June, 1985.
6. McDonnell Aircraft Company Report 83-031, A Natural Formulation for Numerical Solution of the Euler Equations, by A. Verhoff and P.J. O'Neil, 1983.
7. NASA Contractor Report 3712, An Improved Lambda-Scheme for One-Dimensional Flows, by G. Moretti and M.T. DiPiano, 1983.
8. Keenan, J.H., Thermodynamics, John Wiley & Sons, Inc., 1941, p. 88.

INITIAL DISTRIBUTION LIST

	No. Copies
1. Defense Technical Information Center Cameron Station Alexandria, Virginia 22304-6145	2
2. Library, Code 0142 Naval Postgraduate School Monterey, California 93943-5002	2
3. A. Verhoff, Code D341 McDonnell Douglas Corporation Box 516 St. Louis, Missouri 63166-0516	3
4. F. S. Salacka 7 Woodside Road East Apalachin, New York 13732-9428	3
5. Office of Research Administration, Code 012 Naval Postgraduate School Monterey, California 93943-5004	1
6. Chairman, Code 67 Department of Aeronautics Naval Postgraduate School Monterey, California 93943-5004	1
7. Director, Turbopropulsion Laboratory, Code 67Sf Department of Aeronautics Naval Postgraduate School Monterey, California 93943-5004	11
8. Dr. Gerhard Heiche Naval Air Systems Command, Code 03D Washington, D.C. 20361-0001	1
9. Mr. George Derderian Naval Air Systems Command, Code 310E Washington, D.C. 20360-0001	1
10. Dr. M. Keith Ellingsworth Office of Naval Research, Code 1132P 800 North Quincy Street Arlington, Virginia 22217-0001	2

11. Professor Ch. Hirsch 1
Vrije Universiteit Brussel
Pleinlaan 2
1050 Brussels
Belgium
12. Mr. P. Tramm 1
Allison Gas Turbine Division
of General Motors
P.O. Box 420
Indianapolis, Indiana 46206-0420
13. Calvin Ball, Small Gas Turbine Engines 1
NASA Lewis Research Center, MS77-6
21000 Brookpark Road
Cleveland, Ohio 44134-1525
14. David Gordon Wilson 1
M.I.T. Mechanical Engineering, Room 3-455
Cambridge, Massachusetts 02139
15. Helmut E. Weber 1
Professor, Department of
Mechanical Engineering
San Diego State University
San Diego, California 92182-0191
16. Robert Taussig 1
Director, Energy Technology
Spectra Technology, Inc.
2755 Northup Way
Bellevue, Washington 98004-1495
17. Dr. Shmuel Eidelman, Research Physicist 1
Science Application International Co.
1710 Goodridge Dr. Mail Stop G-8-1
McLean, Virginia 22306

215196

Thesis

S15258 Salacka

c.1

Review, implementation and test of the QAZID computational method with a view to wave rotor applications.

215196

Thesis

S15258 Salacka

c.1

Review, implementation and test of the QAZID computational method with a view to wave rotor applications.



thesS15258

Review, implementation and test of the Q



3 2768 000 68453 4

DUDLEY KNOX LIBRARY